

1 **The potential of reed canary grass and the importance of field**
2 **heterogeneity for reducing GHG emissions in a rewetting fen**
3 **peatland**

4 **Andres F. Rodriguez¹, Johannes W.M. Pullens^{1,2}, Jesper R. Christiansen³, Klaus S.**
5 **Larsen³, and Poul E. Lærke^{1,2}**

6 ¹ Department of Agroecology, Aarhus University, Tjele, 8830, Denmark

7 ² iCLIMATE Interdisciplinary Centre for Climate Change, Aarhus University, Roskilde,
8 4000, Denmark

9 ³ Department of Geosciences and Natural Resource Management, University of Copenhagen,
10 Copenhagen, 1958, Denmark

11

12 *Correspondence to:* Andres F. Rodriguez (afrodriguez@agro.au.dk)

13 **Abstract**

14 Rewetting drained peatlands can reduce CO₂ emissions but prevents traditional agriculture.

15 Crop production under rewetted conditions may continue with flood-tolerant crops in

16 paludiculture, but its effects on greenhouse gas (GHG) emissions compared to rewetting

17 without further management are largely unknown. This study was conducted between 2021

18 and 2022 on a fen peatland in central Denmark established with *Phalaris arundinacea* (Reed

19 Canary Grass) ~~(RCG)~~ in 2018. Three harvest/fertilization management treatments (0, 2, and

20 5-cut) were applied with the 2-cut and 5-cut treatments receiving 200 kg N ha⁻¹ y⁻¹ in equal

21 split doses, whereas the 0-cut remained unfertilized. Measurements of CO₂ and CH₄

22 emissions were conducted biweekly under four different light intensities using a manual

23 chamber connected to a gas analyzer. Although the mean annual water table depth (WTD)
24 was -8 cm, indicating a rather wet peatland, the site remained a CO₂ source with a mean net
25 ecosystem C balance ~~of CO₂~~ (NECB) of 6.65 t C ha⁻¹ yr⁻¹ across treatments. Methane
26 emissions averaged 90 kg of CH₄-C ha⁻¹ yr⁻¹, equivalent to 11.7% of NECB given as CO₂
27 equivalents. Results showed that management marginally increased biomass production
28 reflected by more negative gross primary productivity (GPP) in 2-cut and 5-cut compared to
29 0-cut. No significant treatment effect was found on NECB due to field heterogeneity reflected
30 by differences in pore water nutrient concentrations and WTD dynamics among the studied
31 blocks, with higher R_{eco} corresponding to blocks where higher pore water nutrient
32 concentrations were observed. The results indicated that GHG emissions might potentially be
33 reduced when the biomass is harvested from the more productive peatland area in comparison
34 with no management from the more productive peatland area, whereas on the less productive
35 area it might be beneficial to leave the biomass unmanaged. Model simulation of ecosystem
36 respiration (R_{eco}) using WTD data of high temporal resolution captured the variability better
37 as compared to the use of mean annual WTD, which underestimated R_{eco} by 18% on average
38 compared to the hourly WTD model. Data on pore water chemistry further improved
39 statistical linear models of CO₂ fluxes using soil temperature (Ts), WTD, ratio vegetation
40 index (RVI) and photosynthetic active radiation (PAR) as explanatory variables. ~~Significant~~
41 ~~differences in CO₂ emissions and water chemistry parameters were found between studied~~
42 ~~blocks, with higher R_{eco} corresponding to blocks where higher pore water nutrient~~
43 ~~concentrations were present. Methane emissions averaged 90113 kg of CH₄-C ha⁻¹ yr⁻¹,~~
44 ~~equivalent to 121.3% of the total net carbon emission given as CO₂ equivalents.~~ Overall,
45 from a climate perspective the study found that supported paludiculture allowed the
46 production of a biomass production resource in a rewetted agricultural peatland without

47 ~~increasing the carbon emissions footprint~~ compared to no management activity [in rewetted](#)
48 [fertile peatlands](#).

49

50 **1 Introduction**

51 Peatlands are an essential component of the global carbon (C) cycle. Covering only 3% of the
52 terrestrial surface they store ~600 Gt of C, equivalent to 30% of the global soil C pool and
53 exceeding the C stored in vegetation by ~150 Gt (Yu et al., 2010; Scharlemann et al., 2014;
54 Erb et al., 2018; Leifeld and Menichetti, 2018). Northern temperate peatlands can be
55 classified as bogs or fens and store 21.9 Gt C (Leifeld and Menichetti, 2018). While bogs are
56 rain fed and nutrient poor, fens receive drain and ground water from the upland and
57 occasionally from the streams under flooding conditions, making them minerotrophic with a
58 pH close to neutral because the incoming waters carry minerals released from surrounding
59 soils and sediments. Under high nutrient concentrations, fens are dominated by grasses and
60 sedges such as *Phragmites* sp. and *Cladium* sp. (Page and Baird, 2016; Kreyling et al., 2021).

61 Peatland drainage creates aerobic conditions leading to peat mineralization, and consequently
62 soil C is emitted as CO₂ to the atmosphere (Page and Baird, 2016), and dissolved C and
63 [nitrogen \(N\)](#) compounds are leached from the soil (Cabezas et al., 2012; Liu et al., 2019).

64 Emissions from drained peatlands are estimated globally to 785 Mt CO₂ equivalents and the
65 water table is considered the main controlling factor (Zhong et al., 2020; Evans et al., 2021)
66 with higher water tables resulting in lower CO₂ emissions (Tiemeyer et al., 2020; Evans et al.,
67 2021; Koch et al., 2023). However, other factors such as soil temperature (Ts), vegetation,
68 and nutrient status may also affect CO₂ emissions from drained peat soils (Wilson et al.,
69 2016; Rigney et al., 2018; Bockermann et al., 2024). While rewetting reduces CO₂ emissions,
70 it may also lead to increased CH₄ emissions (Wilson et al., 2016; Zhong et al., 2020;

71 Darusman et al., 2023). The CO₂ / CH₄ emission trade-off depends on the water table, the
72 origin of the water (bog/fen), type of vegetation (Rigney et al., 2018; Purre et al., 2019), its
73 nutrient status (Wilson et al., 2016; Tiemeyer et al., 2020), as well as gradual changes in the
74 microbial community following rewetting (Putkinen et al., 2018; Hemes et al., 2019; Emsens
75 et al., 2020; Urbanova and Barta, 2020); However, even considering temporary increases in
76 CH₄ emissions, peatland rewetting and restoration leads to the reestablishment of the C sink
77 function of these ecosystems (Leifeld et al., 2019; Loisel and Gallego-Sala, 2022). Upon
78 drainage, degradation of peat soils is manifested by increases in peat bulk density (Liu et al.,
79 2019; Loisel and Gallego-Sala, 2022), and peat chemistry changes leading to decreasing C:N
80 ratio, humic compounds, and polyphenols, while dissolved organic C (DOC) and N (DON)
81 increase, these changes in peat chemistry may in turn enhance organic matter mineralization
82 (Cabezas et al., 2012; Liu et al., 2019; Zak et al., 2019), and the release of nutrients along
83 with higher bacterial and fungal activity increases CO₂ emissions (AminiTabrizi et al., 2022;
84 Song et al., 2022).

85

86 The importance of peatlands for C storage and GHG emission mitigation, as well as other
87 environmental services, has sparked an interest in peatland restoration with focus on
88 rewetting (Page and Baird, 2016; Andersen et al., 2017). Rewetting can be achieved through
89 different pathways depending on the land use in the peatland after raising the water table.
90 Peatlands have often been rewetted without altering the already established plant community
91 or with the attempt to reestablish the native plant community. Paludiculture has been
92 suggested as an alternative land use, enabling continued agricultural biomass production on
93 the rewetted peatlands under low or high management intensity (Tanneberger et al., 2020;
94 Ziegler, 2020). Paludiculture is expected to reduce CO₂ emissions due to the water-saturated

95 conditions of the peat soils (Ren et al., 2019; Tanneberger et al., 2020; De Jong et al., 2021)
96 while producing biomass for renewable energy such as biogas production (Dragoni et al.,
97 2017; Ren et al., 2019; Hartung et al., 2020) or insulation material that can be used as a green
98 alternative in the building industry (De Jong et al., 2021). Paludiculture may also have the
99 potential to remove excess nutrients from rewetted peatlands by nutrient removal with the
100 harvested biomass (Giannini et al., 2017; Vroom et al., 2018; Geurts et al., 2020).

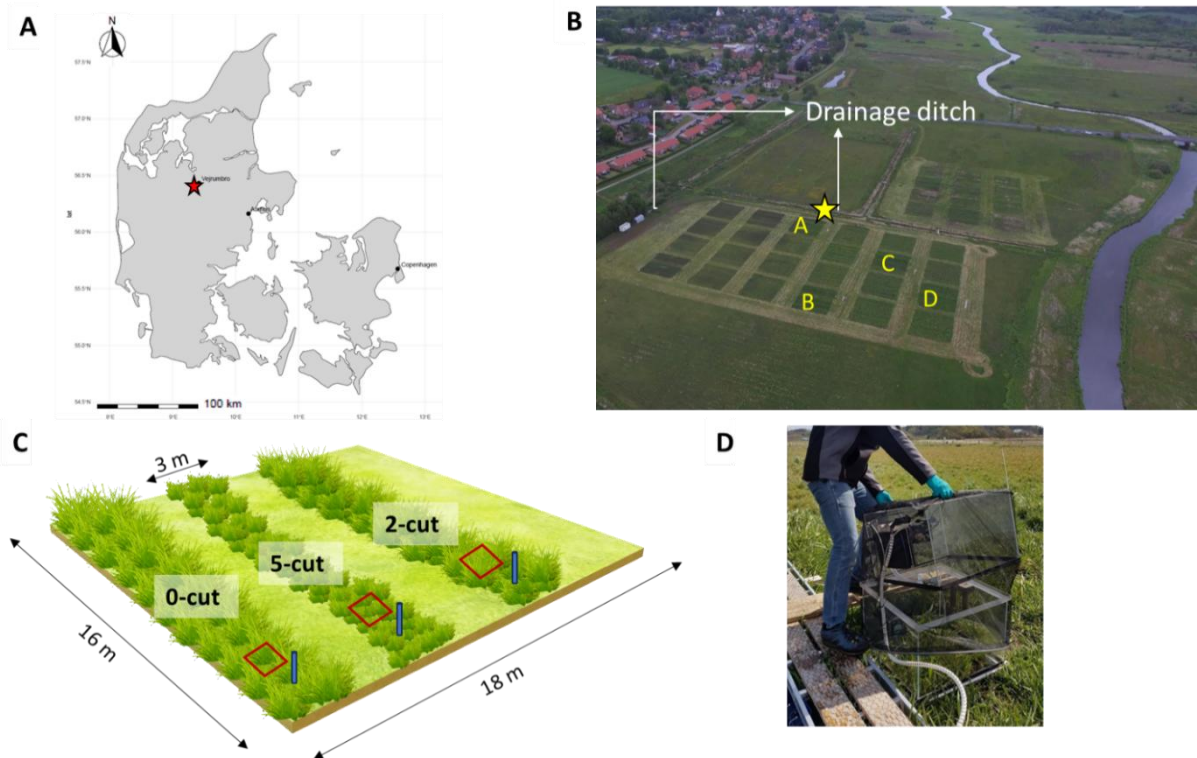
101 Large variation in quantified annual GHG emission from different land use of rewetted
102 peatlands including paludiculture have been reported and further studies are needed to
103 establish emission factors accordingly (Bianchi et al., 2021). It is well accepted that GHGs
104 from rewetted peatlands are influenced by their nutrient content and water table level,
105 reflected by IPCC Tier 1 emissions factors (Wilson et al., 2016). Mean annual water table
106 depth has also been used to predict the net ecosystem carbon balance (NECB), but much
107 uncertainty remains (Tiemeyer et al., 2020; Evans et al., 2021; Koch et al., 2023). The
108 complexity and temporal resolution of gap filling models can also influence the NECB
109 estimates (Karki et al., 2019; Liu et al., 2022) and it is highly uncertain how different
110 management practices, water table dynamics during the year, and nutrient status affect annual
111 emission budgets. Consequently, the objectives of this study were to: (1) determine the ~~C~~CO₂
112 NECB of reed canary grass (RCG) production under three harvest and fertilization
113 management regimes during the third year after establishment in a fen peatland with shallow
114 WTD, (2) assess model performances in gap filling biweekly measurements of ecosystem
115 respiration (R_{eco}) and gross primary productivity (GPP), and (3) investigate the relation of
116 soil water chemistry with R_{eco} and GPP. We hypothesized that, (a) fertilization and harvest of
117 RCG would increase C emissions compared to no RCG management, (b) use of high-
118 temporal frequency data on water table depth (WTD) would improve model prediction of

119 ecosystem respiration (R_{eco}), and (c) knowledge on soil pore water chemistry would improve
120 explanation of C fluxes.

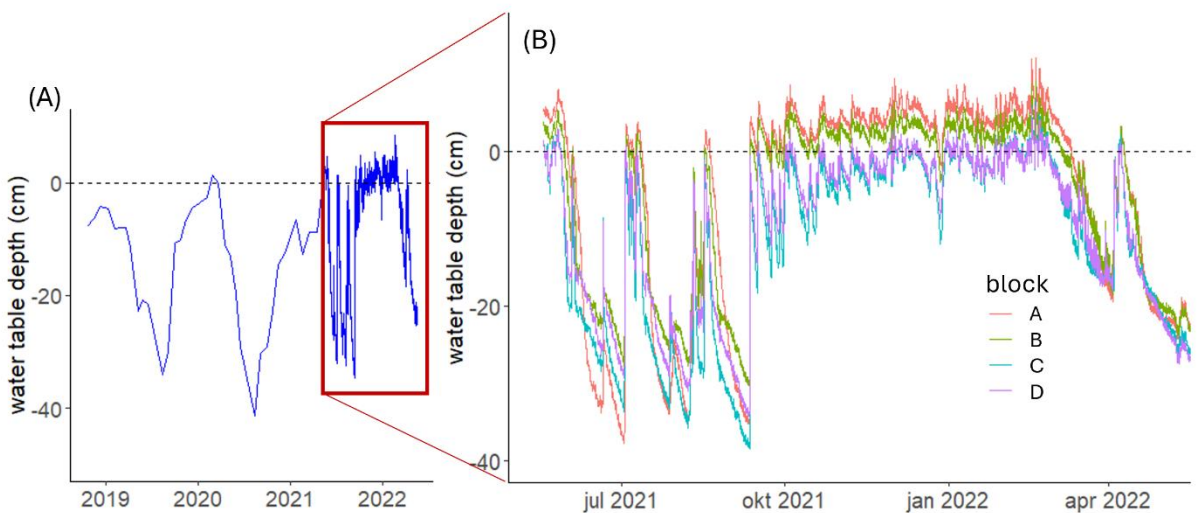
121 **2 Materials and methods**

122 **2.1 Study area**

123 This study was conducted from May 2021 to May 2022 at a riparian fen peatland located in
124 the Nørreå valley, Vejrumbro, Central Jutland, Denmark ($56^{\circ}26'15.3''N$, $9^{\circ}32'44.1''E$) (Fig
125 1). The site was drained in the 1930s and used for agriculture predominantly under grassland
126 rotation and grazing. The field became gradually wetter because of land subsidence, and the
127 water level was largely controlled by the Nørreå stream, located at the southern border of the
128 peatland (Malinowski et al., 2015). After 2018, maintenance of the drainage ditches stopped
129 and the mean annual WTD gradually increased during the following years reaching -8 cm
130 during the study year (18 May 2021 to 17 May 2022), with a minimum of -35 cm in the
131 summer and a maximum of 8 cm in the winter across the experimental blocks (Fig 2a). The
132 mean air temperature and total precipitation during the study year, measured at the
133 Foulumgard meteorological station (Danish Meteorological Institute), located 6 km from the
134 study site, were $9^{\circ}C$ and 709 mm, respectively. The peat layer at the study site has an
135 average depth of 2 m, covering up to 10 m of gyttja (Mashadi et al., 2024). The
136 physicochemical characteristics of the peat at the study area were measured for the top 1
137 meter of the soil as part of a previous study ~~(Table 1)~~ by Nielsen et al. (2023b). Table 1 shows
138 the peat characteristics for the four studied blocks.



139
 140 Figure 1. A, map of Denmark, red star indicates the study site location; B, aerial photograph
 141 of study site, letters indicate the four studied blocks, and yellow star indicates where the ditch
 142 water samples were taken from; C, diagram of one of the blocks showing the three
 143 randomized harvest treatment plots (0-cut, 2-cut, and 5-cut) and the location of collars (red
 144 squares) and piezometers (blue cylinders); D, transparent chamber with shroud used for gas
 145 measurements.



146
 147 Figure 2. Panel (A) presents water table depth (WTD) across the experimental blocks as
 148 measured in each block with intervals of 2-3 weeks at the study site from October 2018 to
 149 April 2021 and every hour from May 2021 until May 2022 (red square). Panel (B) presents
 150 the hourly WTD shown in the red square as the mean of each block with different colors.

151 Table 1. Soil physicochemical characteristics across 0-100 cm depth in the four studied
 152 blocks (A-D).

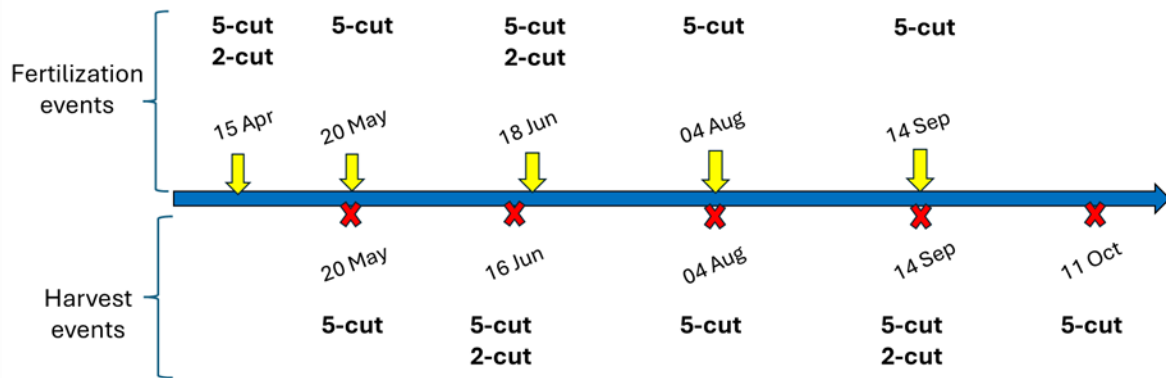
| BlockPlot | OM | pH | ρ_b | TC | TN | C:N |
|------------------|-----------|-----------|----------------------|--------------------|--------------------|------------|
| | % | | g cm ⁻³ | g kg ⁻¹ | g kg ⁻¹ | |
| A | 85 | 5.6 | 0.15 | 440 | 26 | 17 |
| B | 83 | 6.0 | 0.15 | 430 | 28 | 14 |
| C | 70 | 6.2 | 0.18 | 374 | 24 | 15 |
| D | 75 | 6.2 | 0.13 | 401 | 27 | 15 |
| Mean | 78 | 6.0 | 0.15 | 411 | 26 | 15 |

154 †OM, organic matter; ρ_b, bulk density; TC, total C; TN, total N; C:N, carbon to nitrogen
 155 ratio.

157 2.2 Experimental design

158 Four blocks (indicated by A, B, C and D on Fig 1B) were established with reed canary grass
 159 (RCG, *Phalaris arundinacea*, cultivar Lipaula) in 2018 as part of a larger field experiment.
 160 Each block had six randomly placed plots with six different harvest and fertilization
 161 treatments whereof only three (0-cut, 2-cut, 5-cut; referring to the number of harvest events
 162 applied) were used for this study. Thus, the experimental design of this study, which is the
 163 same as Nielsen et al. (2024), consists of four replicate blocks, each with three
 164 harvest/fertilization treatments. Harvest and fertilization dates are shown in Figure 3. The
 165 harvested plots were fertilized with 200 kg N ha⁻¹ and 178 kg K ha⁻¹ in total, given as NPK
 166 18-0-16 in equal split doses. Thus, the 2-cut and the 5-cut received 100 kg N ha⁻¹ and 40 kg N
 167 ha⁻¹ for each cut, respectively, while the 0-cut did not receive any fertilizer. The dimensions
 168 of the blocks and plots were (16 x 18 m), and (16 x 3 m), respectively (Fig 1C). Further
 169 details of the experimental design can be found in Nielsen et al. (2021). At each plot, one 55
 170 x 55 cm collar was installed to 10 cm depth to facilitate closed, non-steady-state chamber
 171 measurements of net CO₂ and CH₄ fluxes. A piezometer with a screen from 5 cm to 100 cm
 172 soil depth was installed 10-20 cm away from the collar at each plot for soil water sampling.
 173 Ts at 5 cm soil depth and WTD were measured continuously at hourly intervals using Ts
 174 dataloggers (HOBO Pendant temperature/light 64K data logger; Onset Corporation,

175 Massachusetts, USA), and Levelloggers (Levellogger 5 Junior; Solinst Canada Ltd, Ontario,
 176 Canada), respectively. Perforated gauge tubes for the levelloggers sealed with lids and soil
 177 temperature loggers were installed in 2020 inside the collars at each plot.



178
 179 Figure 3. Timeline of fertilization and harvest events applied to the 2-cut and 5-cut harvest
 180 treatments during 2021-22.

181

182 **2.3 Net carbon dioxide and methane flux measurements**

183 The CO₂ and CH₄ measurements were performed biweekly +/- one week between 10:00 am
 184 and 3:00 pm on days of predominantly clear sky conditions from 28 May 2021 to 14 June
 185 2022. A total of 26 campaign measurements were undertaken. Fluxes were measured using a
 186 fully transparent chamber (60 cm x 60 cm x 41 cm) made of Plexiglass and equipped inside
 187 with a photosynthetic active radiation (PAR) sensor (190-SA; Li-Cor Inc., Lincoln, NE,
 188 USA), a temperature sensor, and an air mixing fan. Further details of the chamber design and
 189 how the temperature was controlled during operation can be found in Elsgaard et al. (2012).
 190 The chamber was connected to an LGR-ICOS™ GLA131-GGA microportable gas analyzer
 191 (ABB Ltd.), which simultaneously measured water vapor corrected CO₂ and CH₄ (i.e., dry
 192 fractions) at 1 Hz resolution. Chamber deployment was 120 s per measurement. All data were
 193 stored using a Campbell CR1000X data logger (Campbell Sci. Logan, UT, USA) with the
 194 same timestamp. In order to fit the RCG inside the chamber during growth, a chamber

195 extension with the same dimensions as the measurement chamber was used during all
196 measuring campaigns, i.e. total chamber height with the extension was 82 cm. Measurements
197 were conducted during constant PAR conditions, when possible, by timing measurements
198 such that changing cloud conditions were avoided. For each campaign and at each soil collar,
199 fluxes were measured corresponding to four PAR levels by using net shrouds and an opaque
200 cover as described by Kandel et al. (2017). This resulted in four flux measurements, one
201 under fully transparent conditions which corresponded to net ecosystem exchange (NEE), a
202 second under ca. 50% blocked PAR, a third under ca. 75% blocked PAR, and a fourth under
203 100% blocked PAR equivalent to R_{eco} . Between PAR levels plants were given one minute to
204 adapt to the new PAR conditions while the chamber was lifted on one side, allowing air
205 circulation and bringing CO₂ and CH₄ concentrations to atmospheric levels.

206 All fluxes were calculated using the Flux package 0.3-0.1 (Jurasinski et al., 2022) in R (R
207 Core Team (2023), R version 4.3.0). Inspection of fluxes revealed that fluxes were mostly
208 linear, and flux rates were therefore calculated based on linear regression. For low CO₂ fluxes
209 (<100 mg CO₂ m⁻² h⁻¹), fluxes with an $R^2 < 0.6$ and a normalized root mean square error
210 (NRMSE)_{normse} > 0.1 were removed, while for high CO₂ fluxes (>100 mg CO₂ m⁻² h⁻¹),
211 fluxes with an $R^2 < 0.9$ and a NRMSE_{normse} > 0.1 were identified and the PAR and CO₂ flux
212 were manually inspected. If sudden changes in the PAR occurred during the 2 min
213 measurement period or if the flux curve indicated a possible leakage, flux data were
214 discarded. These criteria resulted in 3% of the calculated CO₂ fluxes being removed. In the
215 case of CH₄, ebullitions were excluded by using the *fluxx* function of the Flux package, which
216 automatically detects and excludes rapid concentration fluctuations while calculating fluxes.
217 The resulting calculated linear CH₄ fluxes had R^2 values higher than 0.9, therefore no fluxes
218 were removed based on non-linearity. If a possible leakage was identified by negative or non-
219 linear R_{eco} fluxes, fluxes were removed, resulting in 1.6% of the fluxes removed. For further

220 calculations, only the CH₄ fluxes measured under 100% PAR blocked (opaque conditions)
221 were used.

222 **2.4 Biomass measurements**

223 Spectral reflectance was measured in all collars biweekly at gas sampling days and before
224 and after harvest events using a portable crop sensor (RapidSCAN CS-45; Holland Scientific
225 Inc., Lincoln, NE, USA), which was held 30 cm above the canopy and horizontally rotated
226 45° while performing measurements to cover all vegetation inside the collar. Approximately
227 30 scans were taken per collar and their mean values were used to calculate the ratio
228 vegetation index (RVI) as the ratio between the near-infrared and the red light reflectance.
229 The RVI has been used as a proxy for photosynthetically active biomass and it has been used
230 in photosynthesis and ecosystem respiration models (Kandel et al., 2017; Karki et al., 2019).
231 Hourly RVI values were obtained by linearly interpolating biweekly RVI measurements, and
232 used in GPP and R_{eco} modelling. Fresh weight yield and dry matter content were determined
233 by harvesting the biomass inside the collars at respective cuts and analyzed for total N and C
234 with a Vario Max CN (Elementar Analysensysteme GmbH, Hanau, Germany). Dry matter
235 yields (Table A1) were multiplied by percentage C to obtain the yield in C ha⁻¹ yr⁻¹ as part of
236 the ~~CO₂~~-C budget. The sum of yields from individual cuts per treatment was considered as
237 the annual yield.

238 **2.5 Gap filling models and annual budgets**

239 The measured NEE CO₂ fluxes were partitioned into GPP and R_{eco}. The GPP was calculated
240 for all PAR levels as NEE – R_{eco}. From an atmospheric perspective we always consider R_{eco}
241 positive, and GPP negative while NEE can be either positive (ecosystem carbon source) or
242 negative (ecosystem carbon sink). The net ecosystem carbon balance ~~of CO₂~~-(NECB) was
243 calculated as the sum of the NEE plus the harvested yields for the 2-cut and 5-cut treatments

244 plus the CH₄ emissions. For calculation of annual budgets, three models from previous
 245 studies (one for GPP and two for R_{eco}, see below) were used. Additionally, a fourth model
 246 was developed based on a modification of the two selected R_{eco} models. The GPP was
 247 modelled based on Karki et al. (2019) (model 1).

$$248 \quad GPP = \frac{GPP_{max} * PAR}{k + PAR} * \left(\frac{RVI}{RVI + \alpha} \right) * FT \quad (\text{model 1})$$

249 where GPP is in mg CO₂ m⁻² h⁻¹, *RVI* is the ratio vegetation index, *k* is the PAR value at
 250 which GPP reaches 50%, *α* is a fitted parameter, and *FT* is a linear temperature dependent
 251 function set to 0 when temperature < -2 °C and to 1 when temperature > 10 °C (Kandel et al.
 252 2017).

253 R_{eco} was modelled based on Karki et al. (2019) with *RVI* and *T_s* as input variables (model 2),
 254 based on Rigney et al. (2018) with *WTD* and *T_s* as input variables (model 3), and with a new
 255 model, which included *RVI*, *WTD* and *T_s* as input variables (model 4).

$$256 \quad Reco = t1 + (a * RVI) * e^{\left[b * \left(\frac{1}{T_{10} - T_0} - \frac{1}{T_s - T_0} \right) \right]} \quad (\text{model 2})$$

$$257 \quad Reco = t1 * e^{\left[b * \left(\frac{1}{T_{10} - T_0} - \frac{1}{T_s - T_0} \right) \right]} + (WTD + c)^2 \quad (\text{model 3})$$

$$258 \quad Reco = t1 + (a * RVI) + [(WTD - WTD_{max}) * c]^2 * e^{\left[b * \left(\frac{1}{T_{10} - T_0} - \frac{1}{T_s - T_0} \right) \right]} \quad (\text{model 4})$$

259 where R_{eco} is in mg CO₂ m⁻² h⁻¹, *RVI* is the ratio vegetation index, *WTD* is the water table
 260 depth (cm), *WTD_{max}* is the maximum *WTD* (cm), *t1*, *a*, *b*, and *c* are fitted parameters, *t1* has a
 261 lower limit set at 1, while all other fitted parameters are without upper and lower limits. *T₁₀* is
 262 the reference temperature set to 10 °C, *T₀* is the zero-respiration temperature set to -46 °C,
 263 and *T_s* is the soil temperature (°C) at 5 cm depth.

264
 265 Each R_{eco} model was fitted to data obtained biweekly using non-linear regression (non-least
 266 square) in R (R Core Team (2023), R version 4.3.0) for each plot independently. Annual CO₂
 267 budgets were calculated using the parameterized models, hourly *T_s*, *WTD*, and *RVI*. Model
 268 performance was evaluated by comparing the measured GPP and R_{eco} with the modelled
 269 values using the following indices: Nash-Sutcliffe efficiency, which indicates how well the
 270 plot of observed versus simulated data fits the 1:1 line, with more accurate models having

271 values closer to 1, corrected Akaike information criterion (AICc), normalized root mean
272 square error, and R^2 using the hydroGOF package in R (Zambrano-Bigiarini, 2020). Based on
273 these criteria, the best performing R_{eco} model was used to calculate the annual CO_2 budget. In
274 addition, ~~field~~ models of R_{eco} (model 4) and GPP were parameterized by pooling data from all
275 blocks and treatment plots. ~~The~~ For CH_4 emissions were modelled using model 5 (Karki et al.
276 (2014).); measured fluxes were linearly interpolated to obtain the annual CH_4 budget.

$$CH_4 = (d1 + d2 * WTD) * e^{d3 * Ts} * (d4 + RVI) \quad \text{(model 5)}$$

278 Where WTD is the water table depth, Ts is the soil temperature at 5 cm depth, RVI is the ratio
279 vegetation index, and d1, d2, d3, and d4 are fitted parameters.

280 We tested the sensitivity of the best performing R_{eco} model (model 4) to the frequency of
281 WTD data either using (a) hourly WTD, Ts, and RVI (b) annual mean WTD with hourly Ts
282 and RVI, and (c) annual mean WTD, annual mean Ts, and hourly RVI.

283 **2.6 Water chemistry**

284 Soil pore water was collected biweekly at the same time as the gas campaigns and analyzed
285 for total organic C (TOC), dissolved organic C (DOC), total nitrogen (TN), total dissolved
286 nitrogen (TDN), nitrate-N, (NO_3), ammonia-N (NH_4), total P (TP), total dissolved P (TDP),
287 Fe, pH, ~~electrical~~ conductivity (EC), and turbidity. Pore-water samples were collected
288 immediately after each GHG measurement from the piezometers installed 20 cm from each
289 GHG collar. Water samples were extracted with a syringe from a tube with the other end
290 attached to an aquarium air stone (Air Stone Economy Cylinder 4 X 5 cm, Aquakoi / JV
291 Trading Aps) placed 20 cm below the water table in each piezometer. An additional sample
292 was collected from a ditch draining the peatland. A total of 13 samples were collected per
293 campaign for a total of 338 samples. Upon collection, part of the sample was filtered using

294 0.45 μm pore size filter. The unfiltered samples were analyzed for pH and electrical
295 conductivity (EC) following the Danish Standards DS287 and DS288, respectively,
296 turbidity, TN following Best (1976), TP using the Danish Standard, DS291 photometric
297 method (Dansk Standard, 2004), TOC using a total organic C analyzer (TOC-VCPH;
298 Shimatzu Corporation, Kyoto, Japan), and Fe by ICP emission spectrometer (iCAP 6000
299 series; Thermo Fisher Scientific, Inc., Waltham, Massachusetts, USA). The filtered samples
300 were analysed for DOC with a (TOC-VCPH; Shimatzu Corpotation, Kyoto, Japan), TDN and
301 NO_3 (Best, 1976), TDP by the Danish Standard, DS291 photometric method (Dansk
302 Standard, 2004), and NH_4 following Crooke and Simpson (1971).

303 **2.7 Statistical analysis**

304 Statistics were performed in R (R Core Team (2023), R version 4.3.0). Effects were
305 considered significant if $p \text{ value} < 0.05$. Normality assumptions were evaluated with Q-Q
306 plots, histograms, and residual plots. Kruskal-Wallis tests were used to test the effect of
307 harvest treatment and block on R_{eco} , GPP, NEE, and NECB. Correlations and principal
308 component analysis (PCA) were used to establish relationships between water chemistry
309 parameters, R_{eco} , GPP, NEE, Ts, RVI, PAR, WTD, and CH_4 .

310 ANOVA and Tukey tests were used to determine differences between water chemistry
311 parameters among blocks and harvest treatments. The effects of each water chemistry
312 parameter on R_{eco} and GPP were tested with linear mixed models. Each water chemistry
313 parameter was added one by one as a fixed factor to the base models shown below as models
314 5 and 6, and the performance of the model including each water chemistry parameter was
315 compared to the base model. The R_{eco} base model included WTD, Ts, and RVI as fixed
316 factors and the measuring campaign and replicate block as random factor (model ~~6~~5), while

317 the GPP base model included PAR, Ts, and RVI as fixed factors and measuring campaign and
318 replicate block as random factors (model ~~76~~).

319 $Reco = Harvest\ treatment + WTD + Ts + RVI + (campaign) + (R.Plot)$ (model ~~65~~)

320 $GPP = Harvest\ treatment + PAR + Ts + RVI + (campaign) + (R.Plot)$ (model ~~76~~)

321 Likelihood ratio tests were used to assess if the base models were significantly improved by
322 adding a water chemistry parameter. If this was the case, the R^2 and root mean square error
323 (RMSE) were calculated. Outliers of the water chemistry data were identified as being larger
324 than 3 times the standard deviation for each parameter independently excluding 1% of the
325 data from the analyses.

326 3. Results

327 3.1 Carbon balance

328 Management had a marginally significant effect on GPP (Kruskal-wallis test; p value < 0.1;
329 n: 12), with more negative GPP (larger CO₂ uptake) in the ~~5~~five-cut treatment (-20.2 ± 0.7 t
330 CO₂-C ha⁻¹ yr⁻¹; mean ± SE) and ~~least negative~~lowest in the 0-cut treatment (-15.5 ± 1.3 t
331 CO₂-C ha⁻¹ yr⁻¹) (Table 2). No significant effects of management on R_{eco} (between 22.1 ± 2.5
332 and 22.4 ± 3.3 t CO₂-C ha⁻¹ yr⁻¹; p value = 0.98) and NEE (between 2.2 ± 0.5 and 6.9 ± 2.2 t
333 CO₂-C ha⁻¹ yr⁻¹; p value = 0.22) were registered although the NEE of 0-cut was 4.6 t CO₂-C
334 ha⁻¹ yr⁻¹ higher than the two managed treatments on average. The 2-cut and 5-cut treatments
335 gave similar annual biomass yields (4.0 ± 0.7 and 3.84 ± 0.2 t C ha⁻¹ yr⁻¹, respectively)
336 leading to similar NECB for all treatments when the exported yields ~~and~~ CH₄ were added to
337 the NEE (between 6.10 ± 0.5 and $7.06.9 \pm 2.2$ t CO₂-C ha⁻¹ yr⁻¹). Biomass yields of the 2-cut
338 treatment were similar for both harvesting events, but much lower in block A compared to the
339 other blocks, while for the 5-cut treatment yields peaked at the third harvest and were lowest

340 at the fifth. There were less yield differences between blocks for the 5-cut treatment
341 compared to the 2-cut treatment. Block D had the highest yields of both 2-cut and 5-cut
342 treatments.

343 Although the experimental site looked rather uniform, large differences were foundseen
344 between blocks, especially for Reco and NEE, the latter with coefficients of variation of 0.56,
345 0.71, and 0.41, for the 0-cut, 2-cut, and 5-cut, respectively. The lowest R_{eco} was registered in
346 block A, followed by block B, and the highest R_{eco} was in blocks C and D ($p < 0.05$) (Table 2,
347 Fig 4). Differences in GPP between blocks were not significant despite lower CO_2 uptake
348 leading to lower biomass production in block A. No significant difference in NEE was
349 observed between blocks because the higher R_{eco} was accompanied by larger CO_2 uptake
350 (more negative GPP) and thus higher biomass production. Figure 5 shows that the cumulative
351 NEE grew faster in blocks C and D than in blocks A and B leading to approximately eight
352 times higher annual NEE in blocks C and D compared to block A for the 0-cut treatment. The
353 NECB was marginally different (p value < 0.1) between blocks, with lowest NECB in block
354 A, followed by block B, and highest in block C and D indicating that within field
355 heterogeneity overrides treatments. However, the interaction between treatment and block
356 indicated that harvest of biomass considerably reduced net CO_2 emission in the more
357 productive blocks (C and D) while little effect on NEE was seen for the less productive
358 blocks (A and B) (Figure 5).

359 Cumulated methane emissions averaged 90113 $kg\ CH_4-C\ ha^{-1}\ yr^{-1}$ for the studied year and
360 varied primarily by block with less emissions at block C and largest emissions at block A
361 (Table 23 and Fig. A43). Methane had no significant correlations with nutrients (Fig. A1),
362 except NH_4 , which had a negative correlation with CH_4 . CH_4 also had a positive correlation
363 with R_{eco} and Ts but no significant correlation with WTD.

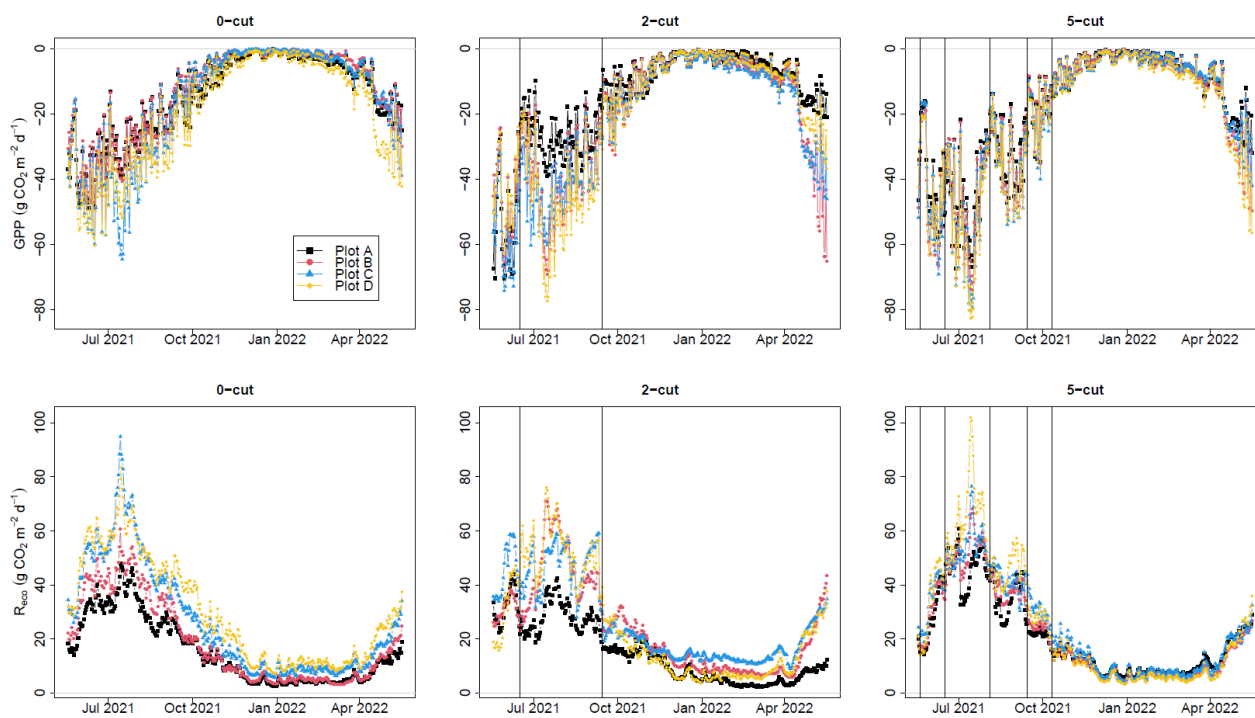
364 Table 2. Cumulated $\text{CO}_2\text{-C}$ emission for the four studied blocks and harvest treatments during
 365 the study year.

| <u>Block</u> | <u>Treatment</u> | <u>Reco</u> t $\text{CO}_2\text{-C ha}^{-1}$ | <u>GPP</u> t $\text{CO}_2\text{-C ha}^{-1}$ | <u>NEE</u> t $\text{CO}_2\text{-C ha}^{-1}$ | <u>Yield</u> t C ha^{-1} | <u>CH₄</u> t $\text{CH}_4\text{-C ha}^{-1}$ | <u>NECB</u> t C ha^{-1} | <u>GWP</u> t $\text{CO}_2\text{e ha}^{-1}$ |
|------------------|------------------|---|--|--|--------------------------------------|---|-------------------------------------|---|
| A | <u>0</u> | 15.4 | -14.2 | 1.2 | NA | 0.15 | 1.3 | 8.9 |
| B | | 18.6 | -13 | 5.6 | NA | 0.10 | 5.7 | 23.5 |
| C | | 26.2 | -16 | 10.2 | NA | 0.03 | 10.2 | 38.3 |
| D | | 29.4 | -18.9 | 10.6 | NA | 0.09 | 10.7 | 41.5 |
| <u>mean ± SE</u> | - | <u>22.4 ± 3.3</u> | <u>-15.5 ± 1.3</u> | <u>6.9 ± 2.2</u> | <u>NA</u> | <u>0.09 ± 0.02</u> | <u>7 ± 2.2</u> | <u>28.1 ± 7.5</u> |
| A | <u>2</u> | 14.9 | -15.3 | -0.4 | 1.9 | 0.12 | 1.6 | 9.1 |
| B | | 23.6 | -20.8 | 2.8 | 4.5 | 0.09 | 7.4 | 29.5 |
| C | | 26.4 | -22 | 4.3 | 4.6 | 0.04 | 9.0 | 34.1 |
| D | | 23.7 | -20.6 | 3.1 | 5 | 0.14 | 8.2 | 34.1 |
| <u>mean ± SE</u> | - | <u>22.1 ± 2.5</u> | <u>-19.7 ± 1.5</u> | <u>2.5 ± 1</u> | <u>4.0 ± 0.7</u> | <u>0.1 ± 0.02</u> | <u>6.6 ± 1.7</u> | <u>26.7 ± 6.0</u> |
| A | <u>5</u> | 20.6 | -18.5 | 2.2 | 3.5 | 0.10 | 5.7 | 23.7 |
| B | | 21 | -20.2 | 0.8 | 3.9 | 0.08 | 4.8 | 19.5 |
| C | | 23.7 | -20.4 | 3.3 | 3.5 | 0.06 | 6.9 | 26.7 |
| D | | 24.3 | -21.9 | 2.4 | 4.5 | 0.06 | 7.0 | 27.1 |
| <u>mean ± SE</u> | - | <u>22.4 ± 0.9</u> | <u>-20.2 ± 0.7</u> | <u>2.2 ± 0.5</u> | <u>3.8 ± 0.2</u> | <u>0.08 ± 0.01</u> | <u>6.1 ± 0.5</u> | <u>24.3 ± 1.8</u> |

366

367 R_{eco} is ecosystem respiration, GPP is gross primary productivity, NEE is net ecosystem
 368 exchange, ~~and~~ NECB ~~of~~ CO_2 is net ecosystem carbon balance (NEE + yield + CH_4), ~~and~~
 369 GWP is the global warming potential (NECB + CH_4) in CO_2 equivalent units.

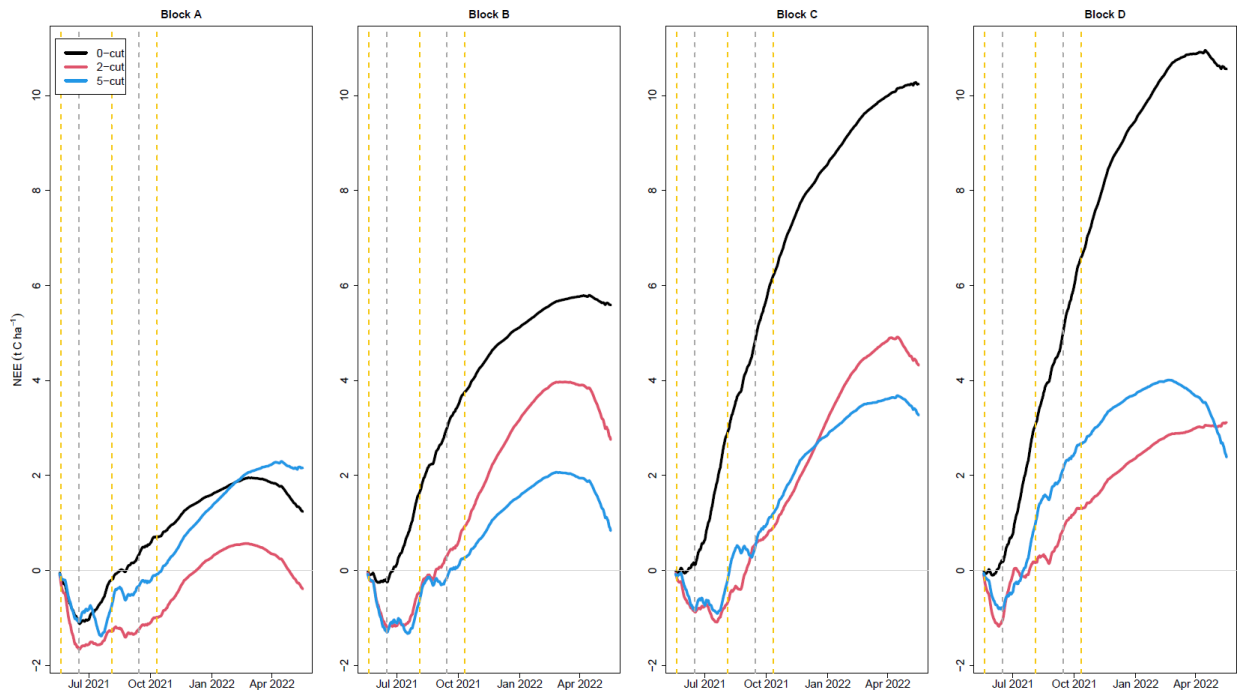
370



371

372 Figure 4. Modelled daily gross primary productivity (GPP) (top) and ecosystem respiration
373 (R_{eco}) (bottom) for the three management treatments (0-cut, 2-cut, and 5-cut). Colors indicate
374 the four block replicates. Vertical lines are harvesting events.

375



376

377 Figure 5. Cumulative net ecosystem exchange for the four studied blocks and three harvest
 378 treatments. Black line is the 0-cut, red line is the 2-cut, and blue line is the 5-cut.
 379 Vertical gray dashed lines are harvest events for only the 2-cut treatment while all vertical
 380 dashed lines are harvest events for both the 2-cut and 5-cut treatments.

381 **Table 3. Cumulated methane emissions for the blocks (A, B, C, D) and harvest treatments 0-**
 382 **cut, 2-cut, and 5-cut during the study year.**

| Block | Treatment | CH ₄ -emissions kg-CH ₄ -ha ⁻¹ |
|-------------------|-----------|--|
| - | - | - |
| A | 0-cut | 200.2 |
| | 2-cut | 157.5 |
| | 5-cut | 125.7 |
| | mean ± SD | 161.1 ± 30.5 |
| B | 0-cut | 124.0 |
| | 2-cut | 129.0 |
| | 5-cut | 99.4 |
| | mean ± SD | 117.5 ± 12.9 |
| C | 0-cut | 35.7 |
| | 2-cut | 40.1 |
| | 5-cut | 73.7 |
| | mean ± SD | 49.8 ± 17 |
| D | 0-cut | 114.5 |
| | 2-cut | 190.0 |
| | 5-cut | 67.6 |
| | mean ± SD | 124.0 ± 50.4 |
| Total mean | | 113.1 |

383 3.2 Model performance

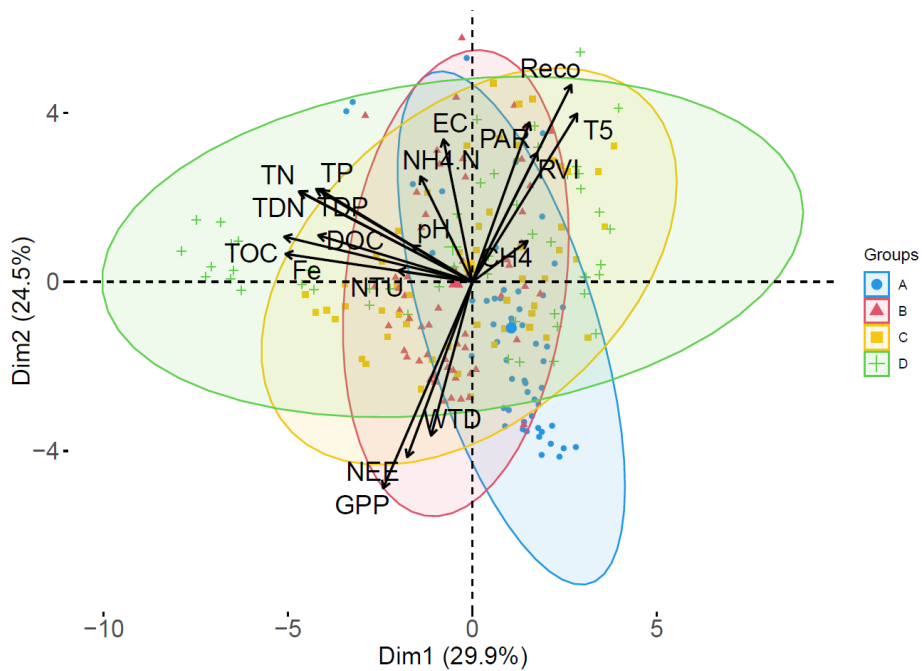
384 Measured R_{eco} was best described by model 4 in 11 out of the 12 studied plots based on the
385 [Nash-Sutcliffe model efficiency \(NSE\)](#) and in 10 out of 12, based on the AICc (table [A34](#)).
386 The other calculated indices (R^2 , and NRMSE) also supported model 4 as the best overall
387 performing model. Additional 1:1 plots of measured vs. modelled R_{eco} for model 4 can be
388 seen in Figure [A32](#) in appendix. When WTD was excluded as seen in model 2 compared to
389 model 4, the overall performance was reduced as indicated by lower NSE for most plots
390 except for plot C 5-cut and plot D 0-cut (Table [A34](#)). Model 3, where RVI was excluded, had
391 the lowest performance of the three tested models. In general, the 0-cut plots provided the
392 best model performances (highest NSE), $R^2 > 0.9$, and the lowest AICc, while the 2-cut and
393 5-cut plots had lower model performances (between 0.74 and 0.92 NSE). The performance
394 results for the GPP models had R^2 values that ranged between 0.81 and 0.96 (Table [A3](#)).
395 R_{eco} was positively correlated with T_s and RVI, and negatively correlated with WTD (lower
396 WTD = deeper water table). On the other hand, GPP was negatively correlated to T_s , RVI,
397 and PAR, meaning that larger T_s , RVI, and PAR correlate to larger CO_2 uptake. These
398 expected relationships seen in the PCA plots (Fig 6) and correlations statistics (Fig. A1)
399 support why the variables in models 1-4 were selected and parameterized in this study. The
400 fitted parameter values of the best performing R_{eco} model and the GPP model varied between
401 plots (Fig [A27](#)). For the R_{eco} model, the b parameter was near its maximum value in most
402 plots, while for the GPP model, the k parameter was near its maximum in most plots.

403 Table 4. Evaluation of three R_{eco} -models parameterized for each plot by four different
 404 performance indices.

405

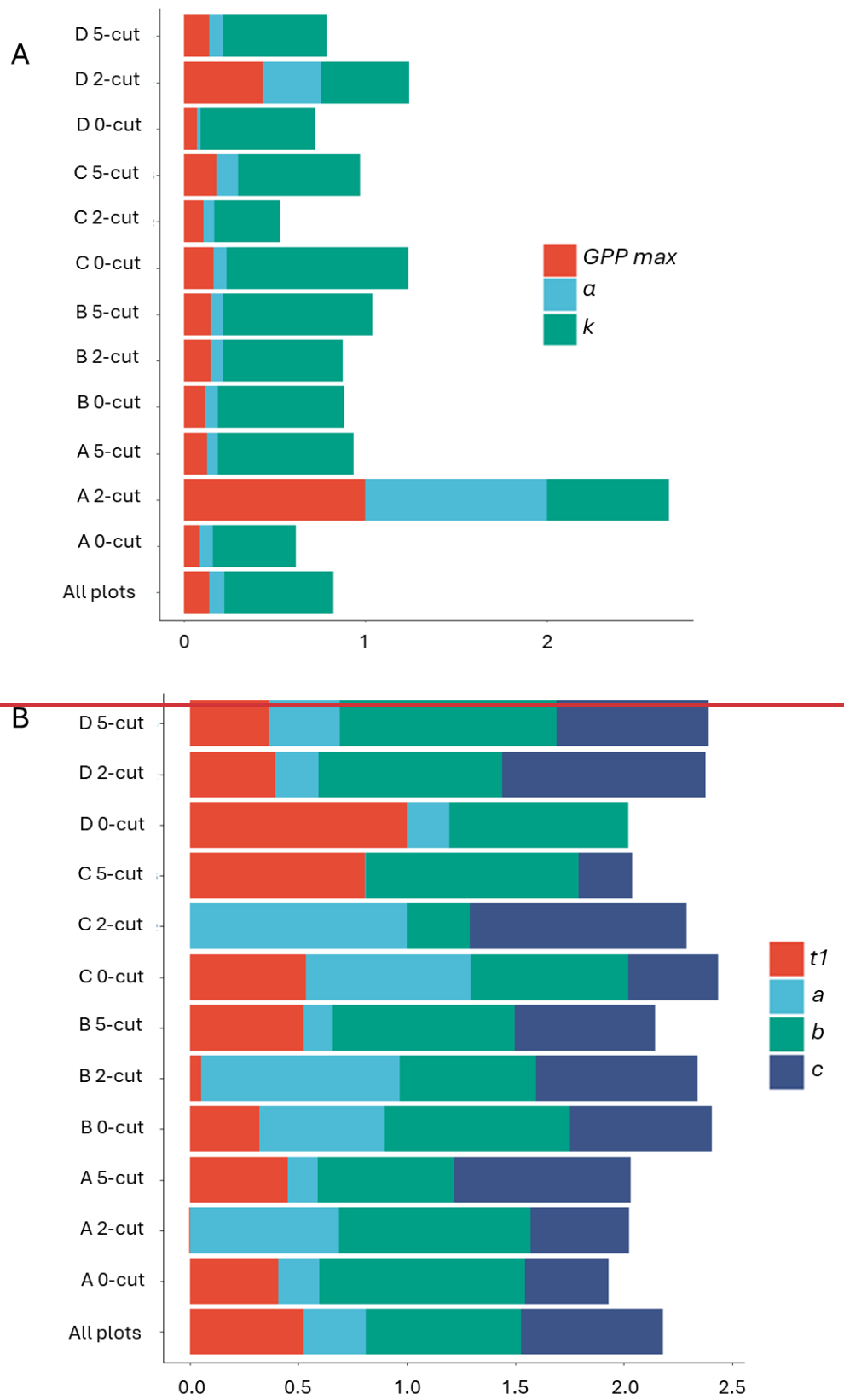
| Block | Treatment | Model 2 | | | | Model 3 | | | | Model 4 | | | |
|-------|-----------|----------------|-------|------|------|----------------|-------|------|------|----------------|-------|------|------|
| | | R ² | NRMSE | NSE | AICc | R ² | NRMSE | NSE | AICc | R ² | NRMSE | NSE | AICc |
| A | 0 | 0.95 | 21.4 | 0.95 | 980 | 0.96 | 19.4 | 0.96 | 1216 | 0.97 | 16.7 | 0.97 | 943 |
| | 2 | 0.85 | 39.2 | 0.84 | 1090 | 0.7 | 54.7 | 0.7 | 1424 | 0.88 | 34.8 | 0.88 | 1073 |
| | 5 | 0.71 | 53.5 | 0.71 | 1247 | 0.84 | 39.9 | 0.84 | 1481 | 0.82 | 42.5 | 0.82 | 1211 |
| B | 0 | 0.95 | 21.6 | 0.95 | 1029 | 0.93 | 26 | 0.93 | 1331 | 0.98 | 15.4 | 0.98 | 978 |
| | 2 | 0.71 | 53.3 | 0.71 | 1261 | 0.67 | 57.4 | 0.67 | 1570 | 0.74 | 50.7 | 0.74 | 1255 |
| | 5 | 0.83 | 40.7 | 0.83 | 1113 | 0.85 | 39 | 0.85 | 1389 | 0.85 | 38.3 | 0.85 | 1106 |
| C | 0 | 0.96 | 19.3 | 0.96 | 1109 | 0.92 | 27.7 | 0.92 | 1446 | 0.96 | 18.7 | 0.96 | 1106 |
| | 2 | 0.77 | 47.8 | 0.77 | 1175 | 0.71 | 53.8 | 0.71 | 1565 | 0.81 | 43.9 | 0.8 | 1163 |
| | 5 | 0.84 | 39.6 | 0.84 | 1227 | 0.84 | 39.9 | 0.84 | 1519 | 0.84 | 39.6 | 0.84 | 1229 |
| D | 0 | 0.9 | 32.1 | 0.9 | 1030 | 0.87 | 36.4 | 0.87 | 1348 | 0.9 | 32.1 | 0.9 | 1032 |
| | 2 | 0.82 | 41.8 | 0.82 | 1229 | 0.81 | 43.3 | 0.81 | 1533 | 0.88 | 34.3 | 0.88 | 1198 |
| | 5 | 0.91 | 31.1 | 0.9 | 1153 | 0.84 | 40.1 | 0.84 | 1484 | 0.92 | 28.5 | 0.92 | 1142 |

406 A, B, C, and D are the four blocks. The three harvest treatments at each block (plots) are 0, 2,
 407 and 5. The four indexes of model evaluation are: R^2 , normalized root mean square of error
 408 (NRMSE), Nash-Sutcliffe efficiency (NSE), and corrected Akaike information criterion
 409 (AICc).



410

411 Figure 6. Principal component analysis PC1 vs PC2 plots. PC1 vs PC2 (A), PC1 vs PC3 (B).
 412 Variability explained by each PCA is the value in parenthesis. Colors represent the four
 413 studied blocks. Harvest treatments are combined.

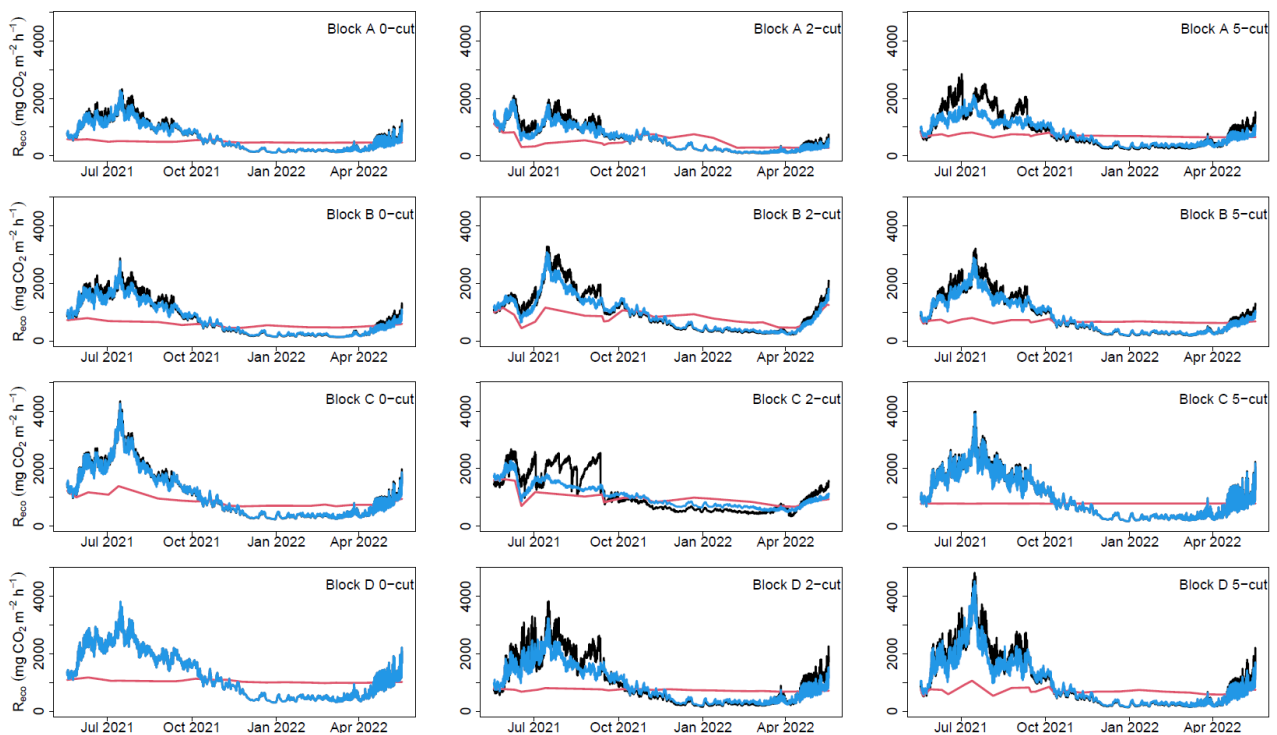


414

415 **Figure 7. Variability of parameters fitted in R_{eeo}-model 4 (A) and the GPP-model (B). Each bar**
 416 **represents a plot, and the bottom bar corresponds to the field model. Each color represents a**
 417 **different parameter. Parameter values were normalized i.e. dividing them by the maximum**
 418 **value:**

419 3.3 Sensitivity analysis using WTD with different temporal resolution

420 Using annual mean WTD and Ts as input for model 4 instead of hourly values,
421 underestimated R_{eco} between 9 to 26% for all plots with an average of 18% (Fig 78) (Table
422 A4). On the other hand, using the annual mean WTD along with hourly Ts generally followed
423 similar trends in R_{eco} as using hourly input data, but high emission events were slightly
424 underestimated resulting in an underestimation that ranged between 0 and 10% with an
425 average of 5% for all plots when compared to the model that used hourly data (Fig 78) (Table
426 A4). If the R_{eco} was calculated using annual mean WTD and annual mean Ts, or annual mean
427 WTD along with hourly Ts, the CO_2 budget resulted in a total mean NECB of 2.76 and 5.43 t
428 $C\ ha^{-1}\ yr^{-1}$, respectively.



429

430 Figure 78. Sensitivity of ecosystem respiration (R_{eco}) modelled for all plots to the data
431 frequency of water table depth (WTD). Black lines represent R_{eco} modelled with hourly
432 WTD, soil temperature (Ts), and RVI, blue line represents R_{eco} modelled with mean annual
433 WTD, hourly Ts, and hourly RVI, and red line represents R_{eco} modelled with mean annual
434 WTD, mean annual Ts, and hourly RVI.

435 3.4 Water chemistry

436 The PCA described in total 67.8 % of the variance in data by the first three principal
437 components. PC1 and PC2 explained 29.9 and 24.7% of the variability in the data,
438 respectively, while PC3 explained 13.4% of the variability ~~(Fig 6)~~. The PC1 VS PC2 plot ~~(Fig~~
439 ~~6)~~ shows clustering of the data with block D and A having the largest difference. PC1
440 describes the pore water nutrients, which are positively correlated with each other, and
441 significance of correlations are presented in Figure A1. This shows that WTD had positive
442 correlations with Fe, TOC and DOC and negative correlations with NH₄ and TDP, while Ts
443 had negative correlations with all nutrients except NH₄ and TDP. Predominant correlations of
444 nutrients with R_{eco} were negative and positive with GPP and NEE, respectively.

445 Comparisons of water chemistry parameters between blocks indicated significant differences
446 depending on type of nutrients. Generally, block (A) had the lowest nutrient concentrations,
447 while block (D) had the highest nutrient concentrations, with the exception of DOC. The
448 nutrient concentrations at the ditch appeared lower than the concentrations in the soil pore
449 water at the blocks except for the TP and TDP (Table ~~35~~). Comparisons between harvest
450 treatments showed that the 2 and 5-cut treatments had higher N and Fe concentrations than
451 the 0-cut treatment, while there were no differences in other nutrients (Table ~~35~~).

452 Additionally, the interaction between harvest treatment and block was significant for NH₄,
453 ~~electrical~~ conductivity, pH, and turbidity.

454 The linear mixed model (Model ~~56~~) indicated that all nutrient concentrations, except NH₄,
455 significantly improved the base R_{eco} model ~~(Table 6)~~, however the effect of TP, TDP, and pH
456 also varied at plot level. For GPP, the addition of nutrients concentrations into the model did
457 not improve the base models, however pH and EC improved model ~~76~~ with its effect varying
458 at plot level. The magnitude of model improvement (higher R² and lower RMSE) was larger
459 for R_{eco} than for GPP, however, in general the R² and RMSE did not change considerably for
460 all nutrients/parameters compared to the base models (Table A5).

461 Table 35. Mean annual concentrations of water chemistry parameters at block A, B, C, and D,
 462 and treatments 0-cut, 2-cut, and 5-cut.

| Block | pH | EC | Turbidity | TOC | DOC | TN | TDN | NH ₄ -N | NO ₃ -N | TP | TDP | Fe |
|------------------|--------------------|---------------------|---------------------|--------------------|--------------------|--------------------|--------------------|---------------------|--------------------|--------------------|--------------------|--------------------|
| | | mS cm ⁻¹ | NTU | mg L ⁻¹ | mg L ⁻¹ | mg L ⁻¹ | mg L ⁻¹ | mg L ⁻¹ | mg L ⁻¹ | mg L ⁻¹ | mg L ⁻¹ | mg L ⁻¹ |
| A | 5.61 ± 0.05 (a) | 0.19 ± 0.01 (a) | 25.4 ± 2.01 (ab) | 164 ± 9 (a) | 129 ± 7 (a) | 14.1 ± 0.9 (a) | 12.8 ± 0.8 (a) | 1.56 ± 0.25 (a) | 4.98 ± 3.18 | 0.49 ± 0.04 (a) | 0.40 ± 0.04 (a) | 12.2 ± 0.9 (a) |
| B | 6.40 ± 0.04 (c) | 0.34 ± 0.01 (c) | 29.6 ± 2.95 (b) | 212 ± 7 (b) | 160 ± 5 (b) | 16.8 ± 0.4 (b) | 15.5 ± 0.5 (b) | 1.50 ± 0.15 (a) | 1.38 ± 0.58 | 0.81 ± 0.04 (c) | 0.69 ± 0.05 (b) | 22.9 ± 1.1 (b) |
| C | 6.22 ± 0.04 (b) | 0.34 ± 0.01 (b) | 40.3 ± 3.76 (c) | 193 ± 10 (b) | 135 ± 6 (ab) | 18.6 ± 0.9 (b) | 16.2 ± 0.7 (b) | 3.34 ± 0.29 (b) | 2.97 ± 1.49 | 0.68 ± 0.04 (b) | 0.50 ± 0.03 (a) | 19.0 ± 1.6 (b) |
| D | 6.25 ± 0.04 (b) | 0.32 ± 0.01 (b) | 26.7 ± 3.85 (a) | 209 ± 16 (b) | 137 ± 8 (a) | 19.6 ± 1.2 (b) | 18.9 ± 1.2 (b) | 2.95 ± 0.24 (b) | 3.58 ± 1.90 | 1.07 ± 0.08 (c) | 0.91 ± 0.08 (b) | 36.3 ± 3.6 (c) |
| ditch | 6.65 ± 0.07 | 0.32 ± 0.01 | 41.9 ± 32.9 | 66 ± 8 | 42 ± 3 | 7.2 ± 1.8 | 4.6 ± 0.3 | 1.2 ± 0.2 | 1.09 ± 0.21 | 1.13 ± 0.23 | 0.93 ± 0.2 | 3.9 ± 1.1 |
| Treatment | | | | | | | | | | | | |
| 0 | 6.13 ± 0.05 (b) | 0.26 ± 0.01 (a) | 27.3 ± 2.4 | 191 ± 9 | 137 ± 5 | 16.0 ± 0.8 (a) | 14.5 ± 0.7 (a) | 1.96 ± 0.16 (a) | 0.15 ± 0.03 | 0.83 ± 0.06 | 0.63 ± 0.05 | 20.3 ± 1.9 (a) |
| 2 | 6.04 ± 0.05 (a) | 0.31 ± 0.01 (b) | 33.3 ± 3.0 | 189 ± 10 | 136 ± 6 | 18.5 ± 0.9 (b) | 16.9 ± 0.9 (b) | 2.69 ± 0.30 (b) | 7.49 ± 2.64 | 0.71 ± 0.04 | 0.59 ± 0.05 | 23.3 ± 1.9 (b) |
| 5 | 6.20 ± 0.04 (b) | 0.33 ± 0.01 (c) | 30.5 ± 3.1 | 203 ± 10 | 148 ± 6 | 17.3 ± 0.7 (ab) | 16.1 ± 0.7 (ab) | 2.36 ± 0.18 (ab) | 1.87 ± 0.49 | 0.76 ± 0.05 | 0.63 ± 0.05 | 24.3 ± 2.2 (ab) |

463

464 Total organic carbon (TOC), dissolved organic carbon (DOC), total nitrogen (TN), total
 465 dissolved nitrogen (TDN), ammonia (NH₄-N), nitrate (NO₃-N), total phosphorus (TP), total
 466 dissolved phosphorus (TDP), electrical conductivity (EC). Values are means ± standard error.
 467 N values are 78, 25, and 104 for the blocks, ditch, and treatments, respectively. Letters in
 468 parenthesis indicate significant differences between block (top) and harvest treatments
 469 (bottom). The ditch was not included in statistical comparisons. No comparisons were
 470 performed for NO₃ due to insufficient data.

471 ~~Table 6. Effect of soil pore water chemistry parameters on ecosystem respiration (R_{eco}, model
 472 5) and gross primary productivity (GPP, model 6).~~

| W.C. Parameter | R _{eco} -effect | GPP-effect |
|-----------------|--------------------------|------------|
| TOC | Sig | Ns |
| DOC | Sig | Ns |
| TN | Sig | Ns |
| TDN | Sig | Ns |
| NH ₄ | Ns | Ns |
| TP | Sig* | Ns |
| TDP | Sig* | Ns |
| Fe | Sig* | Ns |
| pH | Sig* | Sig* |
| Turbidity | Ns | Ns |
| EC | Ns | Sig* |

473

474 ~~Sig indicates significant improvement of the models by individually adding water chemistry
 475 parameters. Sig* indicates a significant effect that varied between harvest treatments. Ns
 476 indicates not significant improvement. Water chemistry parameters included total organic~~

477 carbon (TOC), dissolved organic carbon (DOC), total nitrogen (TN), total dissolved nitrogen
478 (TDN), total phosphorus (TP), total dissolved phosphorus (TDP), and electrical conductivity
479 (EC). N = 312 for all water chemistry parameters.

480

481 4. Discussion

482 4.1 Carbon balance

483 4.1.1 Annual budgets

484 Comparison of results from this study to previous flux measurements on managed Danish
485 peatlands presented by Koch et al. (2023) shows that the total mean CO₂-C emissions (NEE
486 + yield) (NECB) from this study (6.5 ± 2.9 t CO₂-C ha⁻¹ yr⁻¹; ~~mean ± SD~~) are larger than
487 emissions from other Danish organic soils under fertilization and similar WTD (between 0
488 and 2.5 t CO₂-C ha⁻¹ yr⁻¹; Koch et al., 2023). Similarly, our total mean NECB (6.6 t C ha⁻¹ yr⁻¹
489) is larger than emissions from peatlands at similar WTD from both Germany (between -1.0 t
490 C ha⁻¹ yr⁻¹ and 1.5 t C ha⁻¹ yr⁻¹; Tiemeyer et al., 2020) and the UK (between -2.0 t C ha⁻¹ yr⁻¹
491 and 0.8 t C ha⁻¹ yr⁻¹; Evans et al., 2021). ~~Our NECB results are closer to the lower range of~~
492 ~~emissions from drained agricultural peatland presented by Koch et al. (2023).~~ Nielsen et al.
493 (2024) reported the effect of management on GHG emissions from 2020 to 2021 at the same
494 study site as reported here, and found a higher mean NECB of 9.4 t C ha⁻¹ yr⁻¹ at the slightly
495 lower mean annual WTD of -10 cm. Although mean annual WTD increased only 2 cm, not
496 maintaining blocking of the drainage ditches resulted in considerably higher WTD during
497 summer 2021 envisaged by temporary flooded conditions. Higher WTD along with a
498 reduction of WTD fluctuations as rewetting progresses (Karimi et al., 2024), could explain
499 the lower NECB in 2021-22 compared to 2020-21 (Fig 2A). Other studies have also shown a
500 delay in reaching carbon neutral conditions despite drainage being stopped (Hemes et al.,
501 2019; Kreyling et al., 2021). For the shallow annual mean WTD registered at our study site
502 we expected lower CO₂ emission according to IPCC Tier 1 emission factors. However, here

503 R_{eco} is likely driven by the dynamic interaction of a drop in WTD during summer coinciding
504 with maximum T_s . This naturally stimulated CO_2 production in the peat and together with
505 plant respiration drove the high annual R_{eco} (Fig 4).

506 Mean CH_4 emissions from this study were within the range of emissions from pristine and
507 rewetted Danish and German peatlands reported by Koch et al. (2023) and Tiemeyer et al.
508 (2020) (between 75 and 150 kg CH_4 -C ha^{-1} yr^{-1} , approximately) and no treatment effect was
509 apparent. We found that CH_4 emissions contributed 11.7% to total net mean NECB
510 expressed as CO_2e , ~~(using global warming potential (GWP) = 27 for CH_4)~~ (Foster et al.,
511 2021). Peatland rewetting is expected to reduce CO_2 emissions while simultaneously
512 increasing CH_4 emissions (Abdalla et al., 2016; Darusman et al., 2023). Thus, further
513 monitoring of CH_4 emissions would be needed as rewetting progresses at the study site.

514 **4.1.2 Management effect on CO_2 emissions**

515 Rewetted nutrient-rich fen peatlands have higher CO_2 emissions compared to low-nutrient
516 ones (Wilson et al., 2016). Management alternatives to reduce emissions from these sites are
517 therefore needed in order to meet emission reduction targets. Paludiculture has been found to
518 effectively reduce emissions from rewetted peatlands (Tanneberger et al., 2020; De Jong et
519 al., 2021; Bockermann et al., 2024), but type of paludiculture crop seems important for the
520 reduction potential (Lång et al., 2024). Our results showed that after three years of
521 establishment and management of RCG at the study site, NECB was not significantly
522 different compared to no management. These results support findings by Nielsen et al. (2024)
523 who found no effect of management on GHG emissions during the second year (2020) after
524 RCG establishment at the study site. The NECB assumes that all harvested biomass is
525 converted to CO_2 when removed from the field. However, if the biomass is considered as a
526 resource potentially reducing the use of fossil fuels, comparison of NEE among treatments

527 would also be a relevant measure. Based on NEE, we found a potential emission reduction of
528 4.5 and 4.7 t CO₂-C ha⁻¹ yr⁻¹ for the 2 and 5-cut management strategies, respectively, in
529 comparison to no management, but this difference was not significant because of large
530 variation between treatment replicates especially for the 0-cut. Our NEE estimates were
531 lower for all treatments compared to Nielsen et al. (2024). We attribute this reduction in net
532 CO₂ emissions not only to the reduction in biomass production but also to the rewetting
533 process, which lowered heterotrophic peat mineralization.

534 A life cycle assessment of RCG on fen peatlands by Thers et al. (2023) showed that fuel
535 consumption during harvesting can make up a considerable amount of GHG emissions
536 associated to management. Since no considerable difference in yields were found between the
537 2-cut and 5-cut treatments, and a progressive decline was seen after the third harvest of the 5-
538 cut treatment, we would recommend the 2-cut management for RCG in peatlands such as the
539 study site to maximize harvest efficiency and to minimize disturbance to the peatland.

540 Although yields of 2021 (8.9 and 8.6 t DM ha⁻¹) (Table A1) were acceptable they were
541 considerably lower compared to 2019 yields (15.6 and 14.9 t DM ha⁻¹) (Nielsen et al., 2021)
542 and to 2020 yields (12.7 and 13.8 t DM ha⁻¹) (Nielsen et al., 2023a) for the 2-cut and the 5-
543 cut, respectively. The amount of N removed in the harvested biomass was on average 206 kg
544 N ha⁻¹ and slightly lower in the 2-cut compared to the 5-cut (Table A2), therefore, the same
545 amount of N applied as fertilizer was removed at harvest. However, we found generally
546 higher concentrations of N forms in pore water at the 2 and 5-cut treatments compared to the
547 0-cut treatment. A complete assessment of the N balance would help to determine the full
548 environmental benefit of RCG as paludiculture.

549 **4.1.3 Paludiculture and potential CO₂ mitigation**

550 In the most productive blocks of the experiment, paludiculture seemed to accelerate the
551 reducing effect of rewetting on CO₂ emission. Higher R_{eco} and marginally higher NECB were
552 measured in blocks C and D, which in this study were also the areas with higher porewater
553 nutrient concentrations compared to R_{eco} and NECB measured in the block A. The difference
554 in emissions between no harvest (0-cut) and harvest (2 or 5-cut) for the highly productive
555 blocks (C and D) were on average 7.1 t CO₂-C ha⁻¹ yr⁻¹ based on NEE and 2.7 t CO₂-C ha⁻¹
556 yr⁻¹ based on NECB. However, in areas of less emissions (block A in this study),
557 paludiculture would be less recommended because differences were not apparent for
558 harvested and non-harvested plots and relatively small yields could be harvested as a biomass
559 resource. These results stress the importance of acknowledging peatland heterogeneity in
560 rewetting with paludiculture projects to maximize emission reductions.

561 **4.2 Peatland heterogeneity**

562 Even though the studied area was relatively small (3.9 ha) and appeared to be uniform, we
563 found differences in CO₂ emissions and porewater nutrients among the studied blocks. Peat
564 chemistry data (Table 1) also indicated differences in pH, organic matter content, and TC
565 among the studied blocks which might be related to the peat forming process. The peatland
566 heterogeneity might have originated from differences in topography, groundwater flow, and
567 vegetation variability, leading to variable rates of peat and C accumulation (Piilo et al., 2020),
568 and R_{eco} (Juszczak et al., 2013). which affected the pore water nutrient concentrations,
569 microbial communities and GHG balance (Arsenault et al., 2019; Chronakova et al., 2019;
570 Kou et al., 2020). Mashadi et al. (2024) found, at the same location where this study was
571 conducted, an increasing degree of peat decomposition approaching the stream, therefore,
572 higher nutrient concentrations in blocks closer to the stream could be explained by higher
573 peat decomposition and organic matter mineralization at this area. Heterogeneity at the study
574 site was also reflected by considerable variability in values of the fitted parameters of the R_{eco}

575 and GPP models (Fig [A27](#)). Pooling all data to obtain field R_{eco} and GPP models resulted in
576 lower model efficiencies (Table A6) compared to the approach of modelling each plot
577 separately and led to similar R_{eco} , GPP, and NEE among treatments and blocks (Table A7).

578 **4.3 Sensitivity of R_{eco} prediction to temporal resolution of WTD**

579 In previous studies, mean annual WTD have been used as the only predictor for NECB, but
580 not without considerable variation in data points used to build these relationships (Tiemeyer
581 et al., 2020; Evans et al., 2021; Koch et al., 2023). We found that information on Ts, RVI and
582 PAR improved prediction as they have large impact on GPP and R_{eco} . The other two models
583 evaluated (models 2 and 3) also included Ts as explanatory variable. Temperature is a major
584 soil respiration driver (Silvola et al., 1996; Lafleur et al., 2005; Rigney et al., 2018) as higher
585 soil temperatures increase microbial activity and soil respiration but it depends also on water
586 table and soil moisture (Silvola et al., 1996; Lafleur et al., 2005). Out of the three R_{eco} models
587 we tested, the combined model including RVI, WTD and Ts performed best (model 4). When
588 R_{eco} was estimated by models 2 or 3, where either RVI or WTD was omitted the annual R_{eco}
589 and thus NECB was underestimated by 8.9 and 3.5%, respectively. Therefore, model
590 selection is important to accurately estimate CO_2 emissions from peatlands.

591 In this study, Ts captured major trends in R_{eco} . This can be seen by the importance of the
592 fitted Ts parameter (b , model 4) (Fig [A27](#)) and by results shown in Figure [78](#), in which hourly
593 Ts along with mean annual WTD captured most R_{eco} trends, However, this model
594 underestimated R_{eco} by an average of 5%, which would be equivalent to an NECB
595 underestimation of $1.2 \text{ t C ha}^{-1} \text{ yr}^{-1}$ compared to the model with hourly WTD and hourly Ts.
596 The use of mean annual WTD and mean annual Ts resulted in an even larger NECB
597 underestimation ($3.9 \text{ t C ha}^{-1} \text{ yr}^{-1}$) compared to the hourly model. This underestimation is due
598 to the combined effect of lower WTD and higher Ts during summer on R_{eco} , which is not

599 captured when mean WTD and Ts are used. The model based on hourly WTD and Ts also
600 improved simulation of R_{eco} peaks (Figs 8 and A2), which might be of great importance under
601 extreme weather and climate change conditions. Juszczak et al (2013) also found that the
602 response of R_{eco} to Ts can be influenced by WTD and that models including both WTD and
603 Ts provide a better representation of R_{eco} in heterogeneous peatlands. Emission factors
604 derived from models based on annual mean WTD, such as those currently used for rewetted
605 peatlands would underestimate R_{eco} when applied to peatlands with fluctuating and lower
606 WTD during the warm season. This is an important observation particularly for rewetted
607 peatlands, which might take years to achieve hydrological stability (Kreyling et al., 2021).
608 Improved CO_2 modelling therefore requires information on fluctuating WTD possibly
609 obtained from hydrological modelling if measurement data are unavailable.

610 **4.4 Effect of nutrients in CO_2 emissions**

611 Positive correlations between porewater nutrients suggest common drivers for their release.
612 Concentrations of dissolved organic matter components have been found to correlate with
613 concentrations of metals in Canadian bogs (Bourbonniere, 2009). Peat mineralization has
614 been found to be a major driver of nutrient release from drained peatlands (Cabezas et al.,
615 2013; Haapalehto et al., 2014). Predominantly higher nutrient concentrations at the studied
616 blocks compared to the ditch indicate differences between the pore water (measured at the
617 plots) and the groundwater (measured at the ditch), suggesting that peat mineralization and
618 fertilization are larger pore water nutrient sources compared to groundwater. Peat nutrient
619 concentrations and pH have been found to be potential indicators for GHG emissions in
620 rewetting peatlands (Nielsen et al., 2023b). We showed that the prediction of R_{eco} was
621 improved when soil pore water chemistry data were included in addition to WTD, RVI and Ts
622 as fixed factors. Although, the magnitude of this improvement was small based on the R^2
623 increase (between 0.004 and 0.015 depending on the pore water chemistry parameter), this

624 indicated a relation between mineralization and porewater nutrients at the study site. The
625 exact influence of nutrients on R_{eco} should be further investigated. In this study we measured
626 nutrient concentrations but not nutrient load, which is the total mass of a nutrient and can be
627 more informative about the nutrient status of the peatland (Cabezas et al., 2013). Under
628 higher (shallower) WTD, nutrient concentrations can be diluted (Griffiths et al., 2019).
629 Positive correlations between WTD and TOC, DOC and Fe could be due to release of DOC
630 accumulated under drained summer conditions and increase in Fe solubility under higher
631 water tables (Haapalehto et al., 2014).

632 Previous studies have explored variability on water chemistry between and within peatlands
633 (Bourbonniere, 2009; Wood et al., 2016; Arsenault et al., 2018; Griffiths et al., 2019).

634 Nutrient concentrations in peatland's porewater are affected by several factors including
635 water table depth, temperature, peat decomposition degree, and redox (Bourbonniere, 2009;
636 Cabezas et al., 2013; Haapalehto et al., 2014; Wood et al., 2016); Furthermore, nutrient
637 concentrations, base cations, and pH change upon peatland rewetting (Lundin et al., 2017).

638 For this study, WTD was generally lower in blocks C and D (Fig 2B). Malinowski et al.
639 (2015) found that the area where block A is located is more responsive to changes in the
640 stream water level due to its proximity to the drainage ditch, which might have caused the
641 higher mean WTD in this block. Additionally, differences in mobile porosity at the study site
642 might have made some areas more prone to be affected by changes in WTD than others
643 (Mashadi et al., 2024). Minor differences in WTD between the replicate blocks could have
644 produced a different degree of exposure to incoming water sources. Nutrient concentrations
645 in incoming water sources can in turn affect pore water nutrient concentrations (Bridgham
646 and Richardson, 1993; Cabezas et al., 2013), which could have contributed to differences
647 found between blocks, additionally, higher WTD in block A could explain lower nutrient
648 concentrations due to dilution. The minor differences found in WTD might increase peat

649 mineralization in drier blocks resulting in higher DOC and N concentrations (Arsenault et al.,
650 2018; Haapalehto et al., 2014; Wood et al., 2016). Nutrient additions have been found to
651 increase R_{eco} in peat soils (Larmola et al., 2013). Higher mineralization and larger nutrient
652 release from organic matter decomposition at lower WTD blocks could explain differences in
653 CO_2 emissions among replicate blocks as evidenced by higher mineralization and R_{eco} found
654 at blocks C and D. Higher plant productivity and fresh decomposable organic matter
655 contributes to higher nutrient concentrations found in rewetted peatlands (Haapalehto et al.,
656 2014), which could explain higher N concentrations found in blocks C and D. This is also
657 supported by marginally higher NECB found in these blocks compared to blocks A and B (p
658 < 0.1). Nutrients released from the decomposing vegetation have been found to increase soil
659 respiration and mineralization in high-nutrient peat soils (Larmola et al., 2013). A feedback
660 mechanism by which higher mineralization and nutrient release enhances plant productivity,
661 which in turn increases fresh organic matter inputs into the soil and further nutrient releases
662 could drive high nutrient concentrations in poorly drained fen peatlands such as this one.

663 **4.5 Considerations for the potential use of RCG harvested biomass**

664 In order to reestablish the C sink function of rewetted peatlands, peat formation would need
665 to be reestablished, however, reaching this state may take decades (Kreyling et al., 2021).
666 Paludiculture provides an opportunity to achieve indirect GHG emission reductions by
667 replacing fossil fuels, however, since harvested biomass C makes out a considerable amount
668 of GHG emissions from cultivated RCG in fen peatlands because it is considered as a CO_2
669 emission immediately after harvest according to IPCC guidelines (Thers et al., 2023), the end
670 use of the harvested biomass is key to achieve the potential GHG mitigation. Reed canary
671 grass grown in wet Danish fen peatlands was shown suitable for protein extraction as
672 supplement in the diets of monogastric animals and side strips or all the harvested biomass
673 could be used for biogas production thereby replacing fossil fuels (Kandel et al., 2013;

674 Nielsen et al. 2021; Nielsen et al., 2023a). Since N₂O was not measured in the present study,
675 further information is needed to assess the extent of N₂O contribution to GHG emissions
676 given that N fertilization for RCG can increase N₂O emissions in fen peatlands (Kandel et al.,
677 2019), However, N₂O emissions equivalent to 1.4 t CO₂-C_e ha⁻¹ yr⁻¹ was previously reported
678 at the study site without any difference between harvest and non-harvest treatments (Nielsen
679 et al., 2024). The feasibility of using biomass from reed canary grass to offset fossil fuels
680 would depend on the development of non-invasive harvesting techniques, the identification of
681 viable and economically suitable uses for this biomass, and the establishment of markets and
682 infrastructure for its processing.

683

684 5. Conclusion

685 We found that harvesting moderately fertilized RCG in the third production year did not
686 increase net C emissions significantly in poorly drained fen peatlands compared to no
687 management. ~~Additionally, Considering that the climate impact of rewetted sites under~~
688 ~~paludiculture depends on the fate of the harvested biomass, GHG emissions could be reduced~~
689 ~~elsewhere if this biomass is used to replace fossil fuels~~ ~~a biomass resource that potentially~~
690 ~~could reduce GHG emissions elsewhere depending on the end use was produced.~~ When
691 compared with emissions reported earlier for the second production year, the NECB was
692 further reduced in the third production year as rewetting progressed. A main reason for no
693 significant effect of management on NECB was the large differences between treatment
694 replicates which could be partly related to different concentrations of nutrients in pore water
695 and dynamics in WTD across the blocks. Considering theis field heterogeneity, results
696 indicated ed that harvest of the biomass could potentially reduce net C fluxes at nutrient rich
697 areas, while at relatively nutrient poor areas it seemeds more advantageous to leave the grass

698 without management. Paludiculture and management of RCG in rewetting fen peatlands,
699 therefore, offers an alternative that could be particularly beneficial in nutrient rich areas. We
700 found that differences in annual NECB were highly influenced by R_{eco} , and that R_{eco} was best
701 modelled by hourly data on RVI, WTD and Ts. ~~The, with~~ R_{eco} ~~being~~was underestimated when
702 ~~the~~ mean annual WTD was used instead of hourly values, indicating that temporal variability
703 in WTD should be considered in establishing emission factors for rewetted fen peatlands.
704 Differences in porewater nutrient concentrations were able to further improve prediction of
705 R_{eco} based on a statistical model. As more nutrients could be related to higher CO₂ emissions,
706 we suggest a feedback mechanism driving the mineralization, nutrient release, biomass
707 production and peatland heterogeneity. Further research and the establishment of
708 infrastructure and markets for harvested biomass would improve the prospects of
709 paludiculture in rewetted peatlands.

710

711 **Competing interests**

712 The authors declare that they have no conflict of interest.

713

714 **Data availability**

715 Data ~~on~~will CO₂ and CH₄ fluxes as well as pore water nutrient concentrations will be
716 available on Zenodo: <https://doi.org/10.5281/zenodo.14161801>

717

718 **Author contributions**

719 PEL designed the experiment, methodology and directed data collection, AFR, JWMP, and
720 PEL analyzed and visualized the data and wrote the original manuscript, all authors
721 contributed in revising the manuscript.

722

723 **Acknowledgments** The authors would like to acknowledge the following people from the
724 Agroecology Department at Aarhus University, Viborg: Michael Koppelgaard for his help in
725 data collection and processing, Maarit Mäenpää for her help in the statistical analyses,
726 Claudia Nielsen for her help in data processing, and Kirsten Kørup for her help in biomass
727 harvesting.

728 **Funding sources**

729 This study was part of the INSURE project that received funding from the European Joint
730 Programme EJP Soil under the European Union's Horizon 2020 research and innovation with
731 grant agreement no. 862695. Co-funding was received from RePeat DK funded by the Danish
732 Agricultural Agency.

733

734

735 **Appendix A**

736 Table A1. Biomass yields for each harvest event.

| Harvest treatment | Block | Yield per harvest event (t DM ha ⁻¹) | | | | | Total |
|-------------------|-------|--|--------|--------|--------|--------|-------|
| | | 20-May | 16-jun | 04-Aug | 14-sep | 11-Oct | |
| 2 | A | - | 2.8 | - | 1.4 | - | 4.2 |
| 2 | B | - | 5.3 | - | 4.8 | - | 10.1 |
| 2 | C | - | 4.4 | - | 5.8 | - | 10.2 |
| 2 | D | - | 4.6 | - | 6.5 | - | 11.1 |
| 5 | A | 1.5 | 1.5 | 2.9 | 1.4 | 0.5 | 7.8 |
| 5 | B | 1.0 | 2.6 | 3.0 | 1.7 | 0.5 | 8.7 |
| 5 | C | 0.3 | 1.3 | 3.5 | 2.1 | 0.7 | 7.8 |
| 5 | D | 1.2 | 1.9 | 4.2 | 2.0 | 0.7 | 10.1 |

737

738 Table A2. Total N in harvested biomass per event

| Harvest treatment | Block | Total N in biomass per harvest event (kg ha ⁻¹) | | | | | Total |
|-------------------|-------|---|--------|--------|--------|--------|-------|
| | | 20-May | 16-jun | 04-Aug | 14-sep | 11-Oct | |
| 2 | A | - | 62 | - | 31 | - | 93 |
| 2 | B | - | 104 | - | 91 | - | 195 |
| 2 | C | - | 99 | - | 116 | - | 215 |
| 2 | D | - | 91 | - | 113 | - | 204 |
| 5 | A | 49 | 38 | 56 | 40 | 21 | 204 |
| 5 | B | 34 | 61 | 65 | 52 | 20 | 233 |
| 5 | C | 13 | 35 | 93 | 74 | 31 | 245 |
| 5 | D | 41 | 47 | 83 | 59 | 27 | 258 |

739

740

741

742

743

744

745

746

747

748

749

750

751

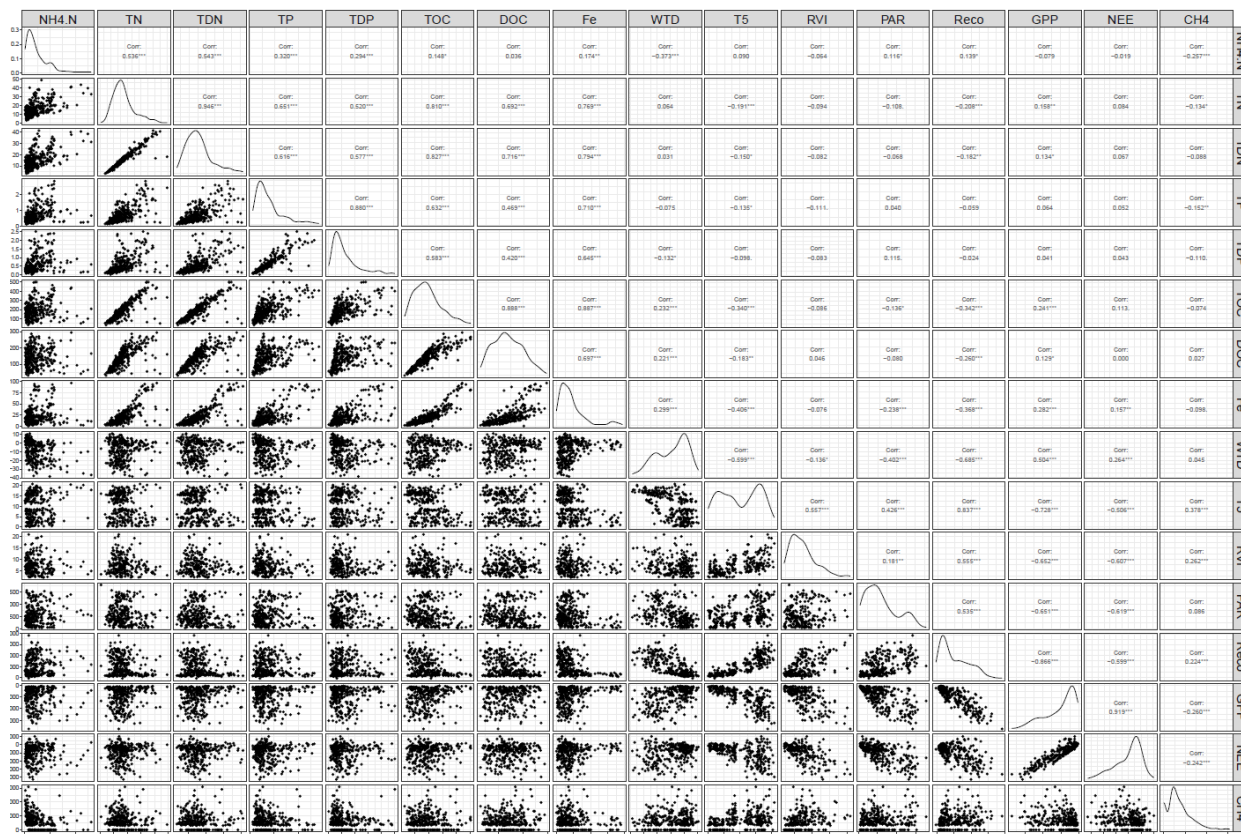
752 Table A3. Model evaluation for GPP model (model 1), R_{eco} models (models 2, 3, and 4), and
 753 CH₄ model (model 5). Values are ~~three different~~ indexes of model performance for each
 754 block.

| BL | T | Model 1 | | | Model 2 | | | | Model 3 | | | | Model 4 | | | | Model 5 | | |
|----|---|----------------|-------|-----|---------|-------|-----|------|---------|-------|-----|------|---------|-------|-----|------|----------------|-------|-------|
| | | R ² | NRMSE | NSE | R2 | NRMSE | NSE | AICc | R2 | NRMSE | NSE | AICc | R2 | NRMSE | NSE | AICc | R ² | NRMSE | NSE |
| A | 0 | 0.9 | 31.1 | 0.9 | 1 | 21.4 | 1 | 980 | 1 | 19.4 | 1 | 1216 | 1 | 16.7 | 1 | 943 | 0.59 | 63.4 | 0.58 |
| | 2 | 0.9 | 24.2 | 0.9 | 0.9 | 39.2 | 0.8 | 1090 | 0.7 | 54.7 | 0.7 | 1424 | 0.9 | 34.8 | 0.9 | 1073 | 0.43 | 74.5 | 0.42 |
| | 5 | 0.9 | 33.9 | 0.9 | 0.7 | 53.5 | 0.7 | 1247 | 0.8 | 39.9 | 0.8 | 1481 | 0.8 | 42.5 | 0.8 | 1211 | 0.41 | 78.0 | 0.37 |
| B | 0 | 0.9 | 29.9 | 0.9 | 1 | 21.6 | 1 | 1029 | 0.9 | 26 | 0.9 | 1331 | 1 | 15.4 | 1 | 978 | 0.49 | 79.5 | 0.34 |
| | 2 | 1 | 19.3 | 1 | 0.7 | 53.3 | 0.7 | 1261 | 0.7 | 57.4 | 0.7 | 1570 | 0.7 | 50.7 | 0.7 | 1255 | 0.11 | 93.1 | 0.10 |
| | 5 | 0.9 | 24.4 | 0.9 | 0.8 | 40.7 | 0.8 | 1113 | 0.9 | 39 | 0.9 | 1389 | 0.9 | 38.3 | 0.9 | 1106 | 0.33 | 80.6 | 0.32 |
| C | 0 | 0.9 | 27.6 | 0.9 | 1 | 19.3 | 1 | 1109 | 0.9 | 27.7 | 0.9 | 1446 | 1 | 18.7 | 1 | 1106 | 0.17 | 93.9 | 0.08 |
| | 2 | 0.8 | 43.4 | 0.8 | 0.8 | 47.8 | 0.8 | 1175 | 0.7 | 53.8 | 0.7 | 1565 | 0.8 | 43.9 | 0.8 | 1163 | 0.03 | 156.4 | -1.55 |
| | 5 | 0.9 | 30.6 | 0.9 | 0.8 | 39.6 | 0.8 | 1227 | 0.8 | 39.9 | 0.8 | 1519 | 0.8 | 39.6 | 0.8 | 1229 | 0.11 | 95.5 | 0.05 |
| D | 0 | 0.9 | 37.5 | 0.9 | 0.9 | 32.1 | 0.9 | 1030 | 0.9 | 36.4 | 0.9 | 1348 | 0.9 | 32.1 | 0.9 | 1032 | 0.49 | 72.7 | 0.45 |
| | 2 | 0.9 | 29.3 | 0.9 | 0.8 | 41.8 | 0.8 | 1229 | 0.8 | 43.3 | 0.8 | 1533 | 0.9 | 34.3 | 0.9 | 1198 | 0.50 | 70.5 | 0.48 |
| | 5 | 0.9 | 32.4 | 0.9 | 0.9 | 31.1 | 0.9 | 1153 | 0.8 | 40.1 | 0.8 | 1484 | 0.9 | 28.5 | 0.9 | 1142 | 0.55 | 72.5 | 0.45 |

755

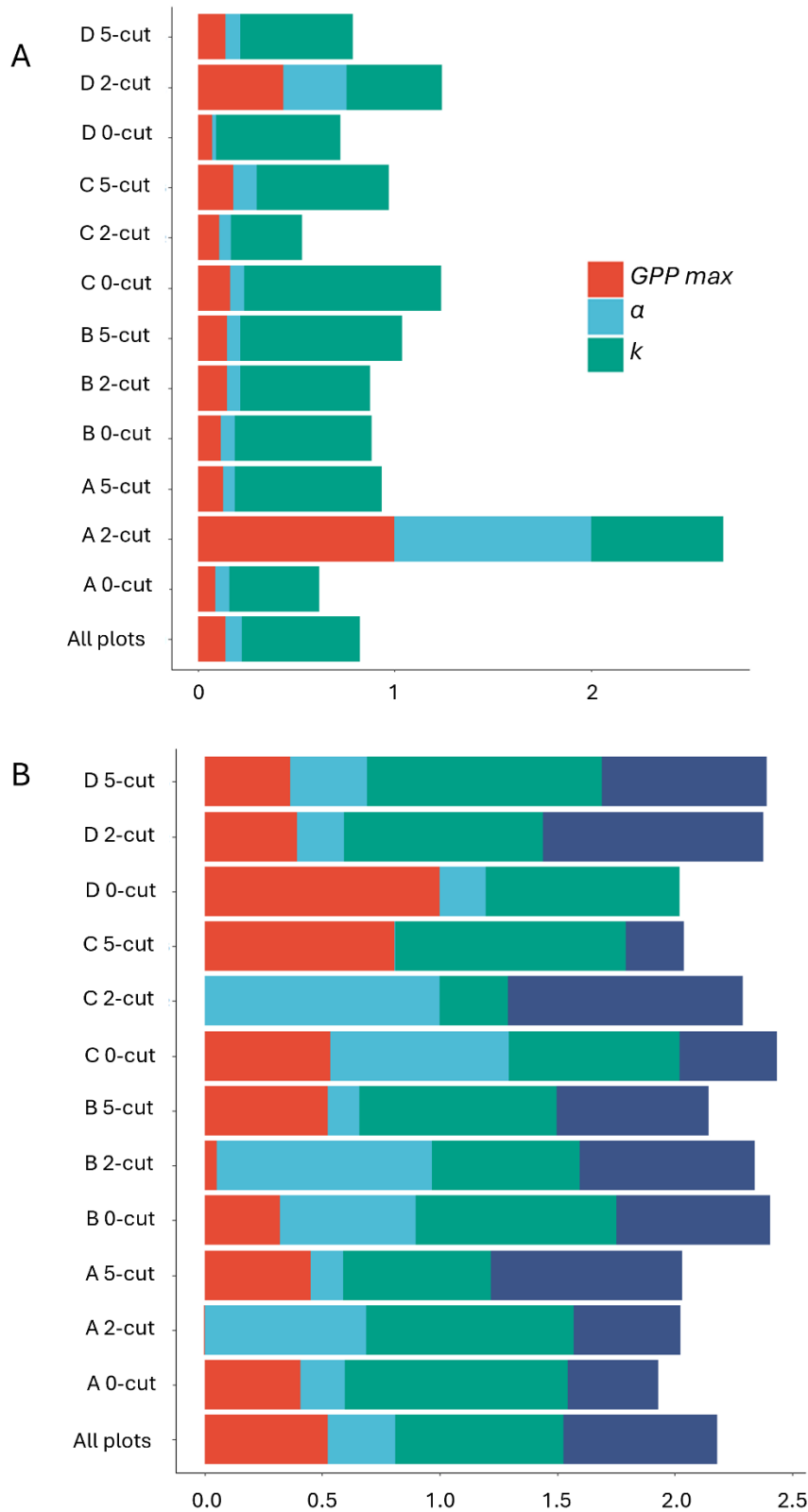
756 A, B, C, and D are the four block replicates, (BL), 0, 2, and 5 are tThe three harvest
 757 treatments (T) at each block ~~are 0, 2, and 5~~. The ~~four~~three indexes of model evaluation are:
 758 R², normalized root mean square of error (NRMSE), ~~and~~ Nash-Sutcliffe efficiency (NSE),
 759 and corrected Akaike Information Criteria (AICc).

760 Figure A1. Pearson's correlations of water chemistry parameters, Ecosystem respiration
 761 (R_{eco}), net ecosystem exchange (NEE), gross primary productivity (GPP), water table depth
 762 (WTD), soil temperature at 5 cm depth (T5), ammonia (NH₄.N), total nitrogen (TN), total
 763 dissolved nitrogen (TDN), total phosphorus (TP), total dissolved phosphorus (TDP), total
 764 organic carbon (TOC), and dissolved organic carbon (DOC). * significant at $p < 0.05$, **
 765 significant at $0.01 > p > 0.001$ *** significant at $p < 0.001$



766
 767
 768
 769
 770
 771
 772
 773
 774
 775
 776
 777
 778

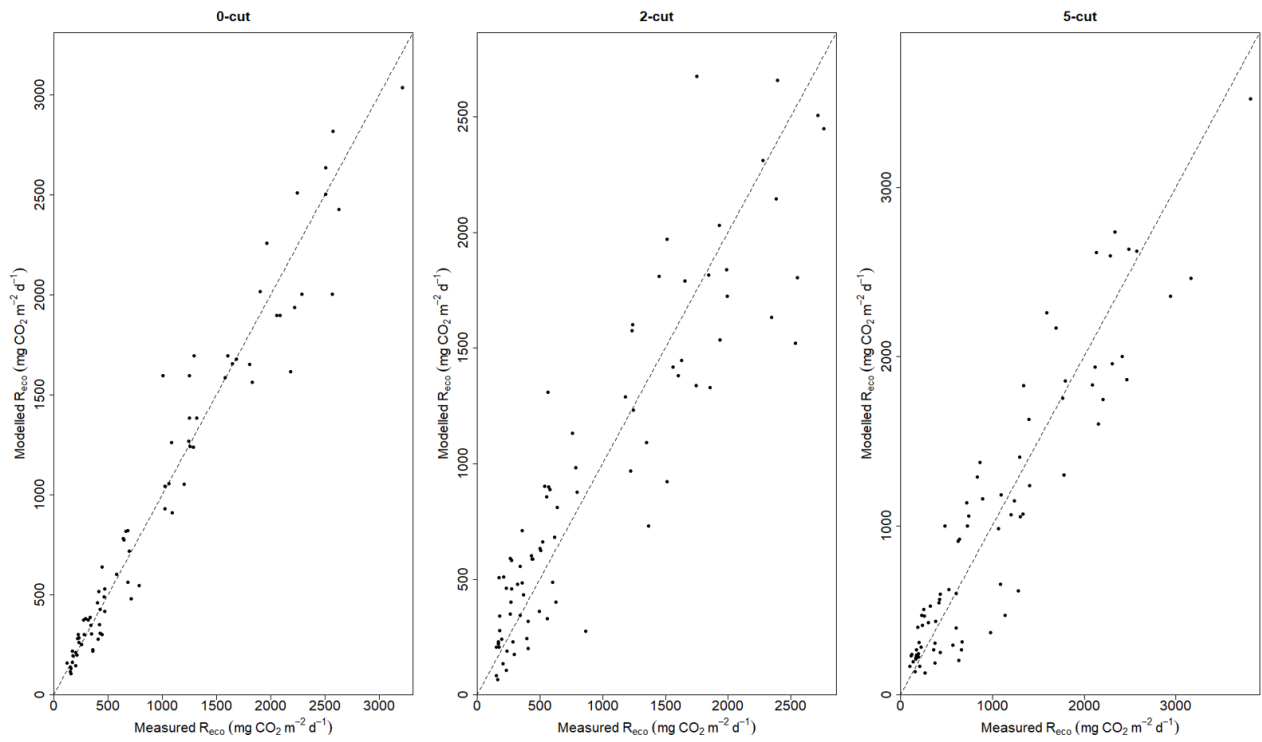
779 **Figure A2. Variability of parameters fitted in R_{eco} model 4 (A) and the GPP model (B). Each bar**
 780 **represents a plot, and the bottom bar corresponds to the model including all plots. Each color**
 781 **represents a different parameter. Parameter values were normalized i.e. dividing them by the**
 782 **maximum value.**



783

784

785 Figure A32. 1:1 plots of measured vs. modelled Reco using model 4 for the three harvest
786 treatments. All blocks are included each of the harvest treatments, N = 104.



787

788

789

790

791

792

793

794

795

796

797

798

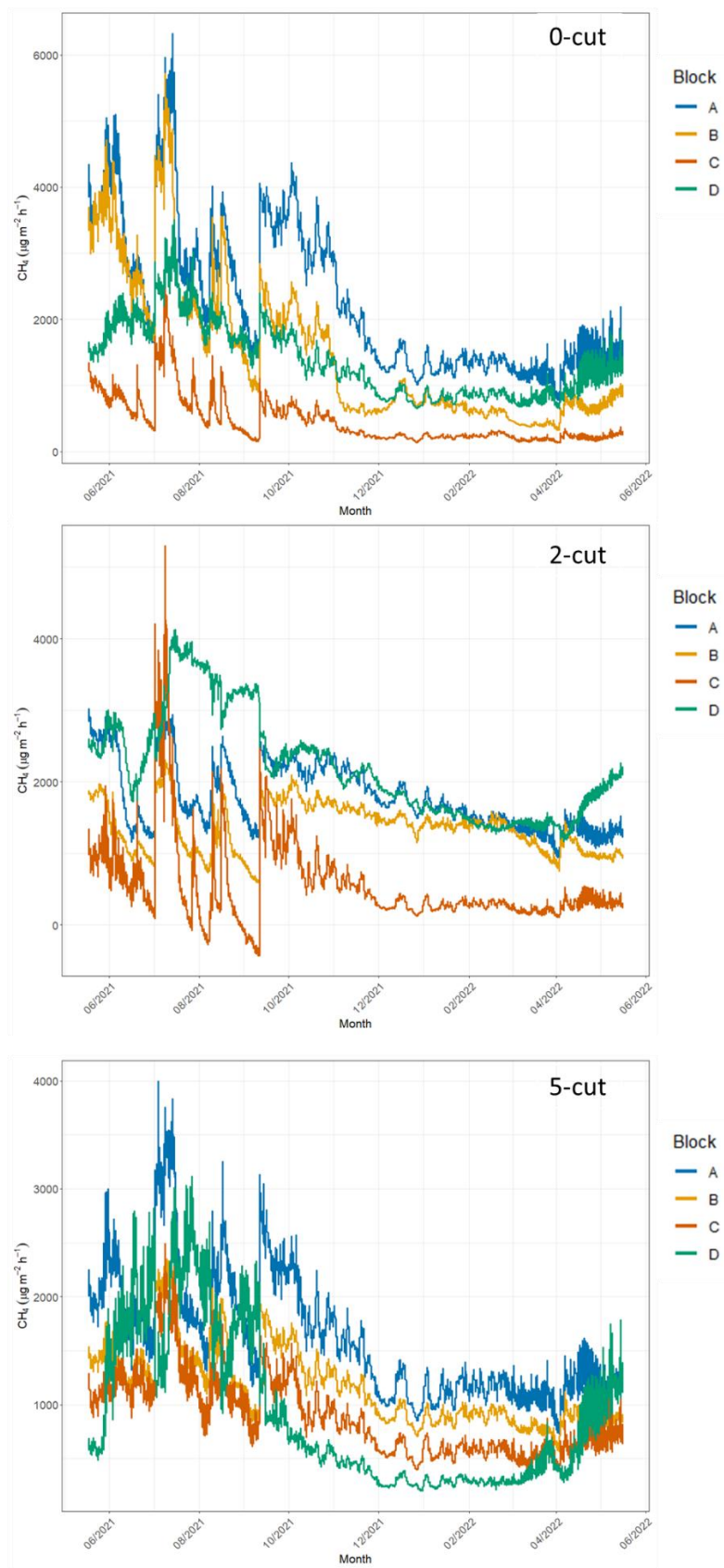
799

800

801

802

803 Figure A43. Time series of methane emissions from studied blocks (different line colors) and
804 from the three harvest treatments (0-cut, 2-cut, and 5-cut). Each dot in the lines represents a
805 measurement campaign. CH₄ emissions calculated only under 0% PAR conditions.



806

807 Table A4. Comparison of annual R_{eco} estimated with models 4, 2 and 3, which use hourly data
 808 on Ts, WTD and RVI, model 4 using either mean annual WTD and Ts (M Model), and model
 809 4 using mean annual WTD and hourly Ts (MH model), the latter two models including hourly
 810 RVI data.

811

| Block | Treatment | Model 4 | Model 2 | Model 3 | M model | MH model |
|--------------|-----------|--|------------|------------|------------|------------|
| | | t CO ₂ -C ha ⁻¹ yr ⁻¹ | | | | |
| A | 0 | 15.4 | 14.9 | 15.4 | 12.2 | 14.8 |
| B | | 18.6 | 18.4 | 18.9 | 14.4 | 17.7 |
| C | | 26.2 | 26.1 | 25.6 | 21.6 | 25.8 |
| D | | 29.4 | 29.4 | 31 | 25.9 | 29.4 |
| Average ± SE | | 22.4 ± 3.3 | 22.2 ± 3.4 | 22.7 ± 3.5 | 18.5 ± 3.2 | 21.9 ± 3.4 |
| A | 2 | 14.9 | 14.5 | 15.1 | 12.3 | 13.9 |
| B | | 23.6 | 23.4 | 23.6 | 20.5 | 22.4 |
| C | | 26.4 | 25.7 | 26 | 24.1 | 24.4 |
| D | | 23.7 | 22.7 | 23 | 18.7 | 21.4 |
| Average ± SE | | 22.1 ± 2.5 | 21.6 ± 2.4 | 21.9 ± 2.4 | 18.9 ± 2.5 | 20.6 ± 2.3 |
| A | 5 | 20.6 | 18.6 | 19.3 | 17.4 | 18.6 |
| B | | 21 | 20.8 | 20.5 | 17.0 | 19.7 |
| C | | 23.7 | 23.6 | 23.4 | 19.8 | 23.4 |
| D | | 24.3 | 22.9 | 23.4 | 17.9 | 22.6 |
| Average ± SE | | 22.4 ± 0.9 | 21.5 ± 1.1 | 21.7 ± 1 | 18 ± 0.6 | 21.1 ± 1.1 |

812

813 Table A5. Total organic carbon (TOC), dissolved organic carbon (DOC), total nitrogen (TN),
 814 total dissolved nitrogen (TDN), total phosphorus (TP), total dissolved phosphorus (TDP),
 815 Turbidity (NTU), electrical conductivity (EC). If base model did not improve by adding the
 816 water chemistry parameters, R² and RMSE are not shown.

817

| Parameter | Reco models | | | | GPP models | | | |
|-----------------|---------------------|-------------------------|-----------|---------------|---------------------|-------------------------|-----------|---------------|
| | Base R ² | Improved R ² | Base RMSE | Improved RMSE | Base R ² | Improved R ² | Base RMSE | Improved RMSE |
| TOC | 0.863 | 0.873 | 243 | 226 | - | - | - | - |
| DOC | 0.863 | 0.871 | 242 | 228 | - | - | - | - |
| TN | 0.863 | 0.870 | 244 | 229 | - | - | - | - |
| TDN | 0.864 | 0.876 | 242 | 224 | - | - | - | - |
| NH ₄ | - | - | - | - | - | - | - | - |
| TP | 0.867 | 0.871 | 241 | 231 | - | - | - | - |
| TDP | 0.862 | 0.867 | 244 | 229 | - | - | - | - |
| FE | 0.863 | 0.878 | 242 | 225 | - | - | - | - |
| pH | 0.863 | 0.868 | 243 | 239 | 0.832 | 0.839 | 645 | 628 |
| NTU | - | - | - | - | - | - | - | - |
| EC | - | - | - | - | 0.832 | 0.839 | 643 | 624 |

818

819 Table A6. Model evaluation of R_{eco} and GPP models using all data pooled and modelling all
820 blocks and harvest treatments all together. ~~“field model”~~

| | | |
|--------------------|-------|----------|
| R_{eco} model | R^2 | 0.78 |
| | NRMSE | 46.6 |
| | NSE | 0.78 |
| | AIC c | 14223.49 |
| GPP model | R^2 | 0.88 |
| | NRMSE | 34.2 |
| | NSE | 0.88 |

821 The four indexes of model evaluation are: R^2 , normalized root mean square of error
822 (NRMSE), Nash-Sutcliffe efficiency (NSE), and corrected Akaike Information Criteria.

823

824 Table A7. Carbon budget results obtained by using all data pooled and modelling all blocks
 825 and harvest treatments all together to obtain ~~field~~ models of R_{eco} and GPP.

| <u>Block</u> | <u>Treatment</u> | <u>Reco</u> t CO ₂ -C ha ⁻¹ | <u>GPP</u> t CO ₂ -C ha ⁻¹ | <u>NEE</u> t CO ₂ -C ha ⁻¹ | <u>Yield</u> t C ha ⁻¹ | <u>CH₄</u> t CH ₄ -C ⁻¹ | <u>NECB</u> t C ha ⁻¹ |
|------------------|------------------|--|---|---|--------------------------------------|---|-------------------------------------|
| <u>A</u> | <u>0-cut</u> | <u>21.1</u> | <u>-16.9</u> | <u>4.2</u> | <u>NA</u> | <u>0.15</u> | <u>4.3</u> |
| <u>B</u> | | <u>18.8</u> | <u>-15.6</u> | <u>3.2</u> | <u>NA</u> | <u>0.10</u> | <u>3.3</u> |
| <u>C</u> | | <u>21.6</u> | <u>-16.6</u> | <u>5.0</u> | <u>NA</u> | <u>0.03</u> | <u>5.1</u> |
| <u>D</u> | | <u>23.0</u> | <u>-19.2</u> | <u>3.8</u> | <u>NA</u> | <u>0.09</u> | <u>3.9</u> |
| <u>Mean ± SE</u> | <u>-</u> | <u>21.1 ± 1.6</u> | <u>-17.1 ± 1.3</u> | <u>4.1 ± 0.7</u> | <u>NA</u> | <u>0.09 ± 0.02</u> | <u>4.2 ± 0.4</u> |
| <u>A</u> | <u>2-cut</u> | <u>21.9</u> | <u>-17.5</u> | <u>4.4</u> | <u>1.9</u> | <u>0.12</u> | <u>6.4</u> |
| <u>B</u> | | <u>22.4</u> | <u>-19.3</u> | <u>3.1</u> | <u>4.5</u> | <u>0.09</u> | <u>7.7</u> |
| <u>C</u> | | <u>23.7</u> | <u>-18.4</u> | <u>5.3</u> | <u>4.6</u> | <u>0.04</u> | <u>10.0</u> |
| <u>D</u> | | <u>22.1</u> | <u>-16.6</u> | <u>5.5</u> | <u>5.0</u> | <u>0.14</u> | <u>10.7</u> |
| <u>Mean ± SE</u> | <u>-</u> | <u>22.6 ± 0.7</u> | <u>-17.9 ± 1</u> | <u>4.6 ± 1</u> | <u>4 ± 0.7</u> | <u>0.1 ± 0.02</u> | <u>8.7 ± 1</u> |
| <u>A</u> | <u>5-cut</u> | <u>23.9</u> | <u>-19.4</u> | <u>4.4</u> | <u>3.5</u> | <u>0.10</u> | <u>8.0</u> |
| <u>B</u> | | <u>23.7</u> | <u>-20.8</u> | <u>2.9</u> | <u>3.9</u> | <u>0.08</u> | <u>6.8</u> |
| <u>C</u> | | <u>25.7</u> | <u>-20.7</u> | <u>5.0</u> | <u>3.5</u> | <u>0.06</u> | <u>8.6</u> |
| <u>D</u> | | <u>23.8</u> | <u>-20.3</u> | <u>3.5</u> | <u>4.5</u> | <u>0.06</u> | <u>8.0</u> |
| <u>Mean ± SE</u> | <u>-</u> | <u>24.3 ± 0.8</u> | <u>-20.3 ± 0.6</u> | <u>3.9 ± 0.8</u> | <u>3.8 ± 0.2</u> | <u>0.08 ± 0.01</u> | <u>7.9 ± 0.4</u> |

826

827 R_{eco} is ecosystem respiration, GPP is gross primary productivity, NEE is net ecosystem
 828 exchange, and NECB ~~of CO₂~~ is the net ecosystem carbon balance (NEE + yield + CH₄).

829

830 **References**

- 831 Abdalla, M., Hastings, A., Truu, J., Espenberg, M., Mander, Ü., & Smith, P. (2016).
832 Emissions of methane from northern peatlands: a review of management impacts and
833 implications for future management options. *Ecology and Evolution*, 6(19), 7080-7102.
- 834 AminiTabrizi, R., Dontsova, K., Grachet, N. G., & Tfaily, M. M. (2022). Elevated
835 temperatures drive abiotic and biotic degradation of organic matter in a peat bog under oxic
836 conditions. *Science of the Total Environment*, 804, 150045.
- 837 Andersen, R., Farrell, C., Graf, M., Muller, F., Calvar, E., Frankard, P., ... & Anderson, P.
838 (2017). An overview of the progress and challenges of peatland restoration in Western
839 Europe. *Restoration Ecology*, 25(2), 271-282.
- 840 Arsenault, J., Talbot, J., & Moore, T. R. (2018). Environmental controls of C, N and P
841 biogeochemistry in peatland pools. *Science of the Total Environment*, 631, 714-722.
- 842 Arsenault, J., Talbot, J., Moore, T. R., Beauvais, M. P., Franssen, J., & Roulet, N. T. (2019).
843 The spatial heterogeneity of vegetation, hydrology and water chemistry in a peatland with
844 open-water pools. *Ecosystems*, 22, 1352-1367.
- 845 Best, E. K. (1976). An automated method for determining nitrate nitrogen in soil
846 extracts. *Queensland Journal of Agricultural and Animal Sciences*. 33, 161-166.
- 847 Bianchi, A., Larmola, T., Kekkonen, H., Saarnio, S., & Lång, K. (2021). Review of
848 greenhouse gas emissions from rewetted agricultural soils. *Wetlands*, 41, 1-7.
- 849 Bockermann, C., Eickenscheidt, T., & Drösler, M. (2024). Adaptation of fen peatlands to
850 climate change: rewetting and management shift can reduce greenhouse gas emissions and
851 offset climate warming effects. *Biogeochemistry*, 1-26.
- 852 Bourbonniere, R. A. (2009). Review of water chemistry research in natural and disturbed
853 peatlands. *Canadian water resources journal*, 34(4), 393-414.
- 854 Bridgham, S. D., & Richardson, C. J. (1993). Hydrology and nutrient gradients in North
855 Carolina peatlands. *Wetlands*, 13, 207-218. Cabezas, A., Gelbrecht, J., Zwirnmann, E., Barth,
856 M., & Zak, D. (2012). Effects of degree of peat decomposition, loading rate and temperature
857 on dissolved nitrogen turnover in rewetted fens. *Soil Biology and Biochemistry*, 48, 182-191.
- 858 Cabezas, A., Gelbrecht, J., & Zak, D. (2013). The effect of rewetting drained fens with
859 nitrate-polluted water on dissolved organic carbon and phosphorus release. *Ecological*
860 *engineering*, 53, 79-88.
- 861 Chroňáková, A., Bárta, J., Kaštovská, E., Urbanová, Z., & Pícek, T. (2019). Spatial
862 heterogeneity of belowground microbial communities linked to peatland microhabitats with
863 different plant dominants. *FEMS Microbiology Ecology*, 95(9), fiz130.
- 864 Croke, W. M., & Simpson, W. E. (1971). Determination of ammonium in Kjeldahl digests of
865 crops by an automated procedure. *Journal of the Science of Food and Agriculture*, 22(1), 9-
866 10.
- 867 Dansk Standard (2004) DS 291. Water Analyses – orthophosphate-phosphorus. Photometric
868 method.

869 Darusman, T., Murdiyarso, D., Impron, & Anas, I. (2023). Effect of rewetting degraded
870 peatlands on carbon fluxes: a meta-analysis. *Mitigation and Adaptation Strategies for Global*
871 *Change*, 28(3), 10.

872 de Jong, M., van Hal, O., Pijlman, J., van Eekeren, N., & Junginger, M. (2021). Paludiculture
873 as paludifuture on Dutch peatlands: An environmental and economic analysis of Typha
874 cultivation and insulation production. *Science of the Total Environment*, 792, 148161.

875 Dragoni, F., Giannini, V., Ragaglini, G., Bonari, E., & Silvestri, N. (2017). Effect of harvest
876 time and frequency on biomass quality and biomethane potential of common reed
877 (*Phragmites australis*) under paludiculture conditions. *BioEnergy research*, 10, 1066-1078.

878 Elsgaard, L., Görres, C. M., Hoffmann, C. C., Blicher-Mathiesen, G., Schelde, K., &
879 Petersen, S. O. (2012). Net ecosystem exchange of CO₂ and carbon balance for eight
880 temperate organic soils under agricultural management. *Agriculture, ecosystems &*
881 *environment*, 162, 52-67.

882 Emsens, W. J., van Diggelen, R., Aggenbach, C. J., Cajthaml, T., Frouz, J., Klimkowska, A.,
883 ... & Verbruggen, E. (2020). Recovery of fen peatland microbiomes and predicted functional
884 profiles after rewetting. *The ISME journal*, 14(7), 1701-1712.

885 Erb, K. H., Kastner, T., Plutzer, C., Bais, A. L. S., Carvalhais, N., Fetzel, T., ... & Luysaert,
886 S. (2018). Unexpectedly large impact of forest management and grazing on global vegetation
887 biomass. *Nature*, 553(7686), 73-76.

888 Evans, C. D., Peacock, M., Baird, A. J., Artz, R. R. E., Burden, A., Callaghan, N., ... &
889 Morrison, R. (2021). Overriding water table control on managed peatland greenhouse gas
890 emissions. *Nature*, 593(7860), 548-552.

891 [Forster, P., Storelvmo, T., Armour, K., Collins, W., Dufresne, J.-L., Frame, D., Lunt, D. J.,](#)
892 [Mauritsen, T., Palmer, M. D., Watanabe, M., Wild, M., & Zhang, H. \(2021\). The Earth's](#)
893 [energy budget, climate feedbacks, and climate sensitivity. In V. Masson-Delmotte, P. Zhai, A.](#)
894 [Pirani, S. L. Connors, C. Péan, S. Berger, N. Caud, Y. Chen, L. Goldfarb, M. I. Gomis, M.](#)
895 [Huang, K. Leitzell, E. Lonnoy, J. B. R. Matthews, T. K. Maycock, T. Waterfield, O. Yelekçi,](#)
896 [R. Yu, & B. Zhou \(Eds.\), *Climate change 2021: The physical science basis. Contribution of*](#)
897 [Working Group I to the Sixth Assessment Report of the Intergovernmental Panel on Climate](#)
898 [Change \(pp. 923–1054\). Cambridge University Press.](#)
899 <https://doi.org/10.1017/9781009157896.009>

900 Geurts, J. J., Oehmke, C., Lambertini, C., Eller, F., Sorrell, B. K., Mandiola, S. R., ... & Fritz,
901 C. (2020). Nutrient removal potential and biomass production by *Phragmites australis* and
902 *Typha latifolia* on European rewetted peat and mineral soils. *Science of the Total*
903 *Environment*, 747, 141102.

904 Giannini, V., Silvestri, N., Dragoni, F., Pistocchi, C., Sabbatini, T., & Bonari, E. (2017).
905 Growth and nutrient uptake of perennial crops in a paludicultural approach in a drained
906 Mediterranean peatland. *Ecological engineering*, 103, 478-487.

907 Görres, C. M., Kutzbach, L., & Elsgaard, L. (2014). Comparative modeling of annual CO₂
908 flux of temperate peat soils under permanent grassland management. *Agriculture, ecosystems*
909 *& environment*, 186, 64-76.

910 Griffiths, N. A., Sebestyen, S. D., & Oleheiser, K. C. (2019). Variation in peatland porewater
911 chemistry over time and space along a bog to fen gradient. *Science of the total*
912 *environment*, 697, 134152.

913 Haapalehto, T., Kotiaho, J. S., Matilainen, R., & Tahvanainen, T. (2014). The effects of long-
914 term drainage and subsequent restoration on water table level and pore water chemistry in
915 boreal peatlands. *Journal of Hydrology*, 519, 1493-1505.

916 Hartung, C., Andrade, D., Dandikas, V., Eickenscheidt, T., Drösler, M., Zollfrank, C., &
917 Heuwinkel, H. (2020). Suitability of paludiculture biomass as biogas substrate— biogas yield
918 and long-term effects on anaerobic digestion. *Renewable energy*, 159, 64-71.

919 Hemes, K. S., Chamberlain, S. D., Eichelmann, E., Anthony, T., Valach, A., Kasak, K., ... &
920 Baldocchi, D. D. (2019). Assessing the carbon and climate benefit of restoring degraded
921 agricultural peat soils to managed wetlands. *Agricultural and Forest Meteorology*, 268, 202-
922 214.

923 Jurasinski G, Koebisch F, Guenther A, Beetz S (2022). `_flux: Flux Rate Calculation from`
924 `Dynamic Closed Chamber Measurements` . R package version 0.3-0.1, <[https://CRAN.R-](https://CRAN.R-project.org/package=_flux)
925 [project.org/package=_flux](https://CRAN.R-project.org/package=_flux)>.

926 Juszczak, R., Humphreys, E., Acosta, M., Michalak-Galczewska, M., Kayzer, D., & Olejnik,
927 J. (2013). Ecosystem respiration in a heterogeneous temperate peatland and its sensitivity to
928 peat temperature and water table depth. *Plant and Soil*, 366, 505-520.

929 Kandel, T. P., Sutaryo, S., Møller, H. B., Jørgensen, U., & Lærke, P. E. (2013). Chemical
930 composition and methane yield of reed canary grass as influenced by harvesting time and
931 harvest frequency. *Bioresource technology*, 130, 659-666.

932 Kandel, T. P., Elsgaard, L., & Lærke, P. E. (2017). Annual balances and extended seasonal
933 modelling of carbon fluxes from a temperate fen cropped to festulolium and tall fescue under
934 two-cut and three-cut harvesting regimes. *GCB Bioenergy*, 9(12), 1690-1706.

935 Kandel, T. P., Karki, S., Elsgaard, L., & Lærke, P. E. (2019). Fertilizer-induced fluxes
936 dominate annual N₂O emissions from a nitrogen-rich temperate fen rewetted for
937 paludiculture. *Nutrient Cycling in Agroecosystems*, 115, 57-67.

938 [Karki, S., Elsgaard, L., Audet, J., & Lærke, P. E. \(2014\). Mitigation of greenhouse gas](#)
939 [emissions from reed canary grass in paludiculture: effect of groundwater level. *Plant and*](#)
940 [Soil](#), 383(1), 217-230.

941 Karimi, S., Hasselquist, E. M., Salimi, S., Järveoja, J., & Laudon, H. (2024). Rewetting
942 impact on the hydrological function of a drained peatland in the boreal landscape. *Journal of*
943 *Hydrology*, 641, 131729.

944 Kreyling, J., Tanneberger, F., Jansen, F., Van Der Linden, S., Aggenbach, C., Blüml, V., ... &
945 Jurasinski, G. (2021). Rewetting does not return drained fen peatlands to their old selves.
946 *Nature communications*, 12(1), 5693.

947 Koch, J., Elsgaard, L., Greve, M. H., Gyldenkerne, S., Hermansen, C., Levin, G., ... &
948 Stisen, S. (2023). Water table driven greenhouse gas emission estimate guides peatland
949 restoration at national scale. *Biogeosciences Discussions*, 2023, 1-28.

950 Kou, D., Virtanen, T., Treat, C. C., Tuovinen, J. P., Räsänen, A., Juutinen, S., ... & Shurpali,
951 N. J. (2022). Peatland heterogeneity impacts on regional carbon flux and its radiative effect
952 within a boreal landscape. *Journal of Geophysical Research: Biogeosciences*, 127(9),
953 e2021JG006774.

954 Lafleur, P. M., Moore, T. R., Roulet, N. T., & Frohling, S. (2005). Ecosystem respiration in a
955 cool temperate bog depends on peat temperature but not water table. *Ecosystems*, 8, 619-629.

956 Larmola, T., Bubier, J. L., Kobylyanec, C., Basiliko, N., Juutinen, S., Humphreys, E., ... &
957 Moore, T. R. (2013). Vegetation feedbacks of nutrient addition lead to a weaker carbon sink
958 in an ombrotrophic bog. *Global Change Biology*, 19(12), 3729-3739.

959 Leifeld, J., & Menichetti, L. (2018). The underappreciated potential of peatlands in global
960 climate change mitigation strategies. *Nature communications*, 9(1), 1071.

961 Leifeld, J., Wüst-Galley, C., & Page, S. (2019). Intact and managed peatland soils as a source
962 and sink of GHGs from 1850 to 2100. *Nature Climate Change*, 9(12), 945-947.

963 Liu, H., Zak, D., Rezanezhad, F., & Lennartz, B. (2019). Soil degradation determines release
964 of nitrous oxide and dissolved organic carbon from peatlands. *Environmental Research
965 Letters*, 14(9), 094009.

966 Liu, W., Fritz, C., Weideveld, S. T., Aben, R. C., Van Den Berg, M., & Velthuis, M. (2022).
967 Annual CO₂ budget estimation from chamber-based flux measurements on intensively
968 drained peat meadows: Effect of gap-filling strategies. *Frontiers in Environmental
969 Science*, 10, 803746.

970 Loisel, J., & Gallego-Sala, A. (2022). Ecological resilience of restored peatlands to climate
971 change. *Communications Earth & Environment*, 3(1), 208.

972 Lundin, L., Nilsson, T., Jordan, S., Lode, E., & Strömberg, M. (2017). Impacts of rewetting
973 on peat, hydrology and water chemical composition over 15 years in two finished peat
974 extraction areas in Sweden. *Wetlands ecology and management*, 25, 405-419.

975 Lång, K., Honkanen, H., Heikkinen, J., Saarnio, S., Larmola, T., & Kekkonen, H. (2024).
976 Impact of crop type on the greenhouse gas (GHG) emissions of a rewetted cultivated
977 peatland. *Soil*, 10(2), 827-841.

978 Malinowski, R., Groom, G., Schwanghart, W., & Heckrath, G. (2015). Detection and
979 delineation of localized flooding from WorldView-2 multispectral data. *Remote
980 sensing*, 7(11), 14853-14875.

981 Mashhadi, S. R., Grombacher, D., Zak, D., Lærke, P. E., Andersen, H. E., Hoffmann, C. C., &
982 Petersen, R. J. (2024). Borehole nuclear magnetic resonance as a promising 3D mapping tool
983 in peatland studies. *Geoderma*, 443, 116814.

984 Nielsen, C. K., Stødkilde, L., Jørgensen, U., & Lærke, P. E. (2021). Effects of harvest and
985 fertilization frequency on protein yield and extractability from flood-tolerant perennial
986 grasses cultivated on a fen peatland. *Frontiers in Environmental Science*, 9, 619258.

- 987 Nielsen, C. K., Stødkilde, L., Jørgensen, U., & Lærke, P. E. (2023a). Ratio vegetation indices
988 have the potential to predict extractable protein yields in green protein paludiculture. *Mires &*
989 *Peat*, (29).
- 990 Nielsen, C. K., Elsgaard, L., Jørgensen, U., & Lærke, P. E. (2023b). Soil greenhouse gas
991 emissions from drained and rewetted agricultural bare peat mesocosms are linked to
992 geochemistry. *Science of the Total Environment*, 896, 165083.
- 993 Nielsen, C. K., Liu, W., Koppelgaard, M., & Lærke, P. E. (2024). To Harvest or not to
994 Harvest: Management Intensity did not Affect Greenhouse Gas Balances of Phalaris
995 Arundinacea Paludiculture. *Wetlands*, 44(6), 79.
- 996 Page, S. E., & Baird, A. J. (2016). Peatlands and global change: response and
997 resilience. *Annual Review of Environment and Resources*, 41, 35-57.
- 998 Piilo, S. R., Korhola, A., Heiskanen, L., Tuovinen, J. P., Aurela, M., Juutinen, S., ... &
999 Väiliranta, M. M. (2020). Spatially varying peatland initiation, Holocene development, carbon
1000 accumulation patterns and radiative forcing within a subarctic fen. *Quaternary Science*
1001 *Reviews*, 248, 106596.
- 1002 Purre, A. H., Penttilä, T., Ojanen, P., Minkkinen, K., Aurela, M., Lohila, A., & Ilomets, M.
1003 (2019). Carbon dioxide fluxes and vegetation structure in rewetted and pristine peatlands in
1004 Finland and Estonia. *Boreal Environment Research*.
- 1005 Putkinen, A., Tuittila, E. S., Siljanen, H. M., Bodrossy, L., & Fritze, H. (2018). Recovery of
1006 methane turnover and the associated microbial communities in restored cutover peatlands is
1007 strongly linked with increasing Sphagnum abundance. *Soil Biology and Biochemistry*, 116,
1008 110-119.
- 1009 R Core Team (2023). *_R: A Language and Environment for Statistical Computing_*. R
1010 Foundation for Statistical Computing, Vienna, Austria. <<https://www.R-project.org/>>.
- 1011 Ren, L., Eller, F., Lambertini, C., Guo, W. Y., Brix, H., & Sorrell, B. K. (2019). Assessing
1012 nutrient responses and biomass quality for selection of appropriate paludiculture
1013 crops. *Science of the Total Environment*, 664, 1150-1161.
- 1014 Scharlemann, J. P., Tanner, E. V., Hiederer, R., & Kapos, V. (2014). Global soil carbon:
1015 understanding and managing the largest terrestrial carbon pool. *Carbon management*, 5(1),
1016 81-91.
- 1017 Silvola, J., Alm, J., Ahlholm, U., Nykanen, H., & Martikainen, P. J. (1996). CO₂ fluxes from
1018 peat in boreal mires under varying temperature and moisture conditions. *Journal of ecology*,
1019 219-228.
- 1020 Rigney, C., Wilson, D., Renou-Wilson, F., Müller, C., Moser, G., & Byrne¹, K. A. (2018).
1021 Greenhouse gas emissions from two rewetted peatlands previously managed for forestry.
1022 *Mires and Peat*, 21, 1-23.
- 1023 Song, Y., Cheng, X., Song, C., Li, M., Gao, S., Liu, Z., ... & Wang, X. (2022). Soil CO₂ and
1024 N₂O emissions and microbial abundances altered by temperature rise and nitrogen addition in
1025 active-layer soils of permafrost peatland. *Frontiers in Microbiology*, 13, 1093487.

- 1026 Tanneberger, F., Schröder, C., Hohlbein, M., Lenschow, U., Permien, T., Wichmann, S., &
 1027 Wichtmann, W. (2020). Climate change mitigation through land use on rewetted peatlands–
 1028 cross-sectoral spatial planning for paludiculture in Northeast Germany. *Wetlands*, *40*(6),
 1029 2309-2320.
- 1030 Thers, H., Knudsen, M. T., & Lærke, P. E. (2023). Comparison of GHG emissions from
 1031 annual crops in rotation on drained temperate agricultural peatland with production of reed
 1032 canary grass in paludiculture using an LCA approach. *Heliyon*, *9*(6).
- 1033 Tiemeyer, B., Freibauer, A., Borraz, E. A., Augustin, J., Bechtold, M., Beetz, S., ... & Drösler,
 1034 M. (2020). A new methodology for organic soils in national greenhouse gas inventories: Data
 1035 synthesis, derivation and application. *Ecological Indicators*, *109*, 105838.
- 1036 Urbanová, Z., & Bárta, J. (2020). Recovery of methanogenic community and its activity in
 1037 long-term drained peatlands after rewetting. *Ecological engineering*, *150*, 105852.
- 1038 Vroom, R. J., Xie, F., Geurts, J. J., Chojnowska, A., Smolders, A. J., Lamers, L. P., & Fritz, C.
 1039 (2018). *Typha latifolia* paludiculture effectively improves water quality and reduces
 1040 greenhouse gas emissions in rewetted peatlands. *Ecological engineering*, *124*, 88-98.
- 1041 Wilson, D., Blain, D., Couwenberg, J., Evans, C. D., Murdiyarso, D., Page, S., ... & Tuittila,
 1042 E. S. (2016). Greenhouse gas emission factors associated with rewetting of organic soils.
 1043 *Mires and Peat*, *17*, 1-28.
- 1044 Wood, M. E., Macrae, M. L., Strack, M., Price, J. S., Osko, T. J., & Petrone, R. M. (2016).
 1045 Spatial variation in nutrient dynamics among five different peatland types in the Alberta oil
 1046 sands region. *Ecohydrology*, *9*(4), 688-699.
- 1047 Yu, Z., Loisel, J., Brosseau, D. P., Beilman, D. W., & Hunt, S. J. (2010). Global peatland
 1048 dynamics since the Last Glacial Maximum. *Geophysical research letters*, *37*(13).
- 1049 Zak, D., Roth, C., Unger, V., Goldhammer, T., Fenner, N., Freeman, C., & Jurasinski, G.
 1050 (2019). Unraveling the importance of polyphenols for microbial carbon mineralization in
 1051 rewetted riparian peatlands. *Frontiers in Environmental Science*, *7*, 147.
- 1052 Zambrano-Bigiarini, M. (2020) hydroGOF: Goodness-of-fit functions for comparison of
 1053 simulated and observed hydrological time series, R package version 0.4-0. URL
 1054 <https://github.com/hzambran/hydroGOF>. DOI:10.5281/zenodo.839854.
- 1055 Zhong, Y., Jiang, M., & Middleton, B. A. (2020). Effects of water level alteration on carbon
 1056 cycling in peatlands. *Ecosystem Health and Sustainability*, *6*(1), 1806113.
- 1057 Ziegler, R. (2020). Paludiculture as a critical sustainability innovation mission. *Research*
 1058 *Policy*, *49*(5), 103979.